

Hybrids of coumarin-indole: Design, synthesis and biological evaluation in triton WR-1339 and high-fat diet induced hyperlipidemic rat models

Koneni V. Sashidhara,^{*a} K. Bhaskara Rao,^{§a} Ravi Sonkar,^{§b} Ram K. Modukuri,^a Yashpal S. Chhonker,^c Pragati Kushwaha,^a Hardik Chandasana,^c A. K. Khanna,^b Rabi S. Bhatta,^c Gitika Bhatia,^b Manish Kumar Suthar,^b Jitendra Kumar Saxena,^b Vikash Kumar,^d Mohammad Imran Siddiqi.^d

^a*Medicinal and Process Chemistry Division, and ^bDivision of Microbiology, CSIR-Central Drug Research Institute, BS-10/1, Sector 10, Jankipuram extension, Sitapur Road, Lucknow 226031, India.*

^b *Biochemistry Division, CSIR-Central Drug Research Institute, BS-10/1, Sector 10, Jankipuram Extension, Sitapur Road, Lucknow 226031, India.*

^c*Pharmacokinetics and Metabolism Division, CSIR-Central Drug Research Institute, BS-10/1, Sector 10, Jankipuram Extension, Sitapur Road, Lucknow 226031, India*

^d*Division of Molecular and Structural Biology, CSIR-Central Drug Research Institute, BS-10/1, Sector 10, Jankipuram Extension, Sitapur Road, Lucknow 226031, India*

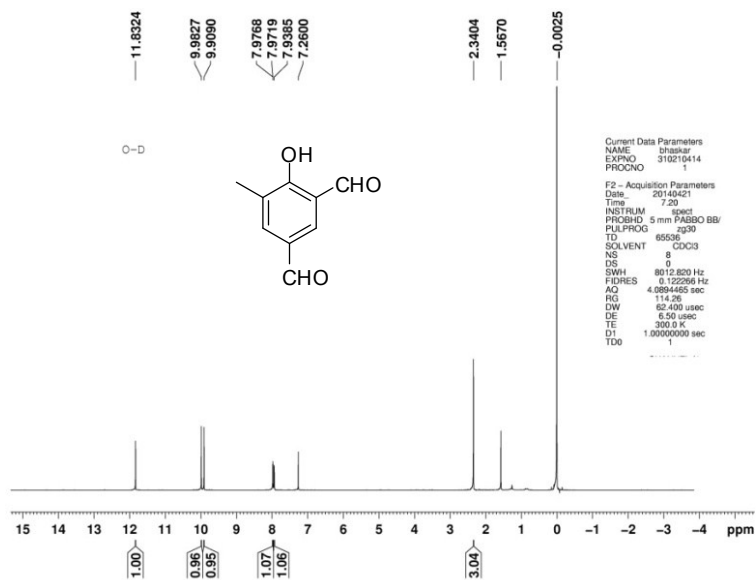
*Corresponding author. Tel.: +91 9919317940; Fax: +91-522-2628493.

§These authors contributed equally.

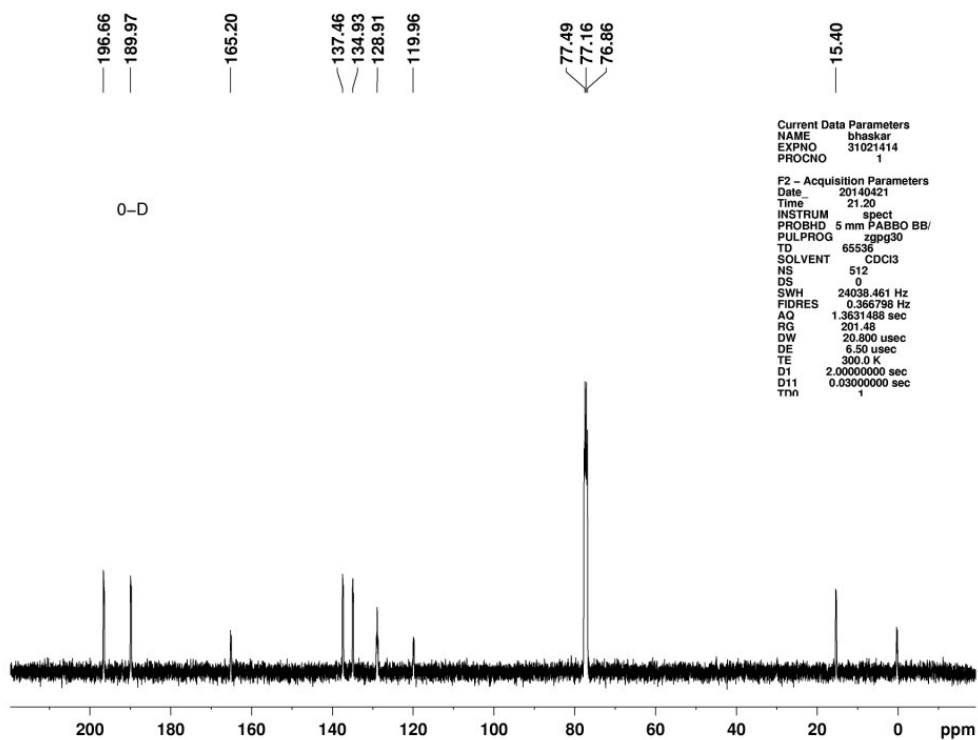
Email: kv_sashidhara@cdri.res.in, sashidhar123@gmail.com (Dr. K. V. Sashidhara)

1. Compounds NMR Spectra

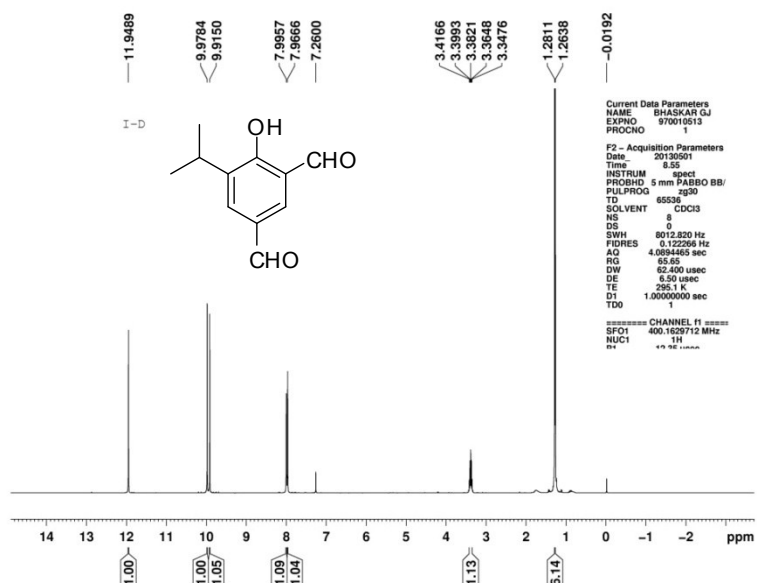
^1H NMR of compound **5** at 400 MHz (CDCl_3)



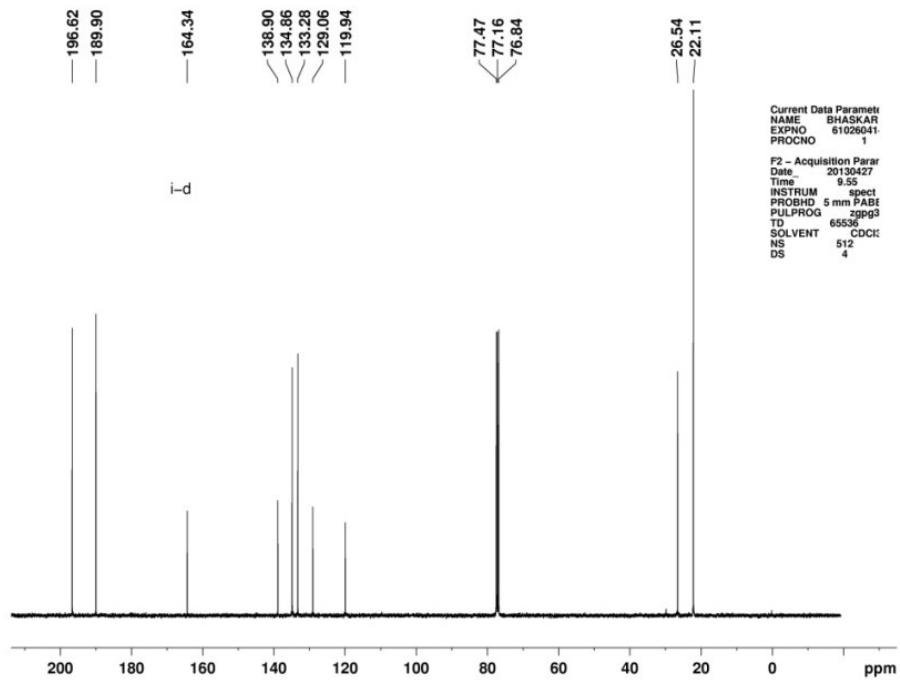
^{13}C NMR of compound **5** at 100 MHz (CDCl_3)



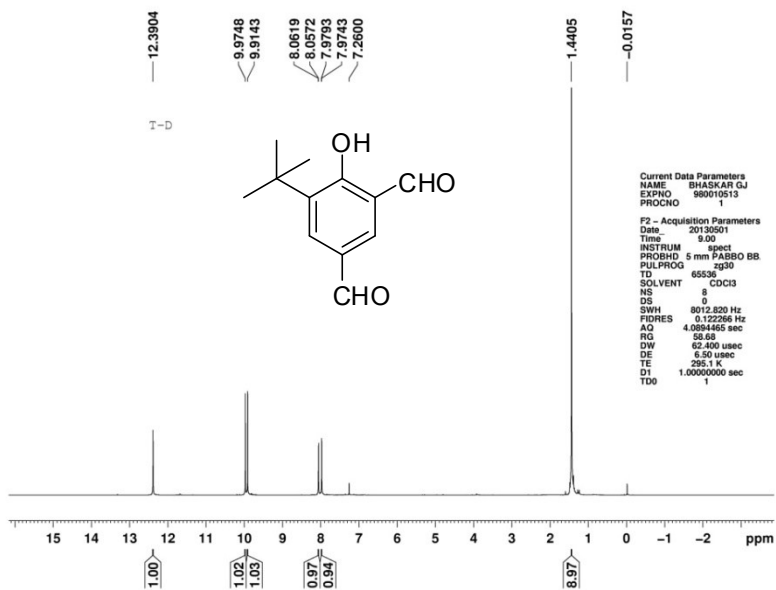
^1H NMR of compound **6** at 400 MHz (CDCl_3)



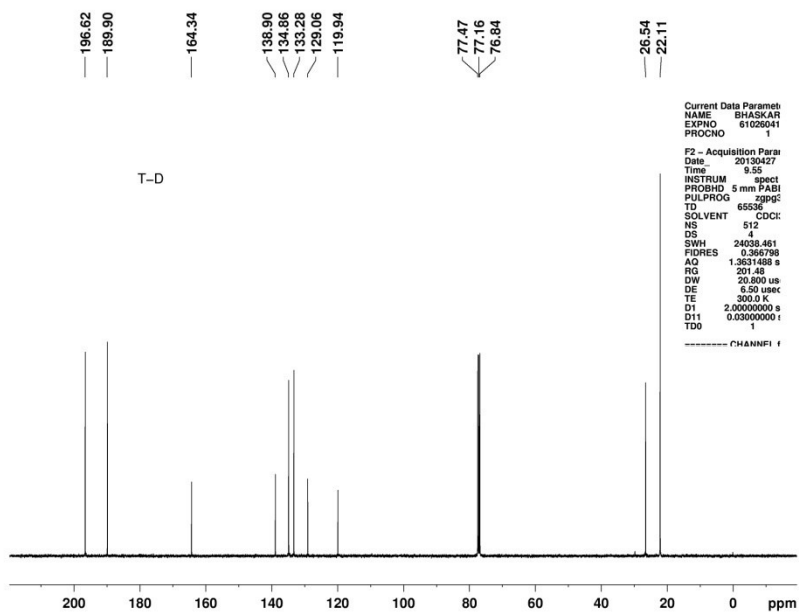
^{13}C NMR of compound **6** at 75 MHz (CDCl_3)



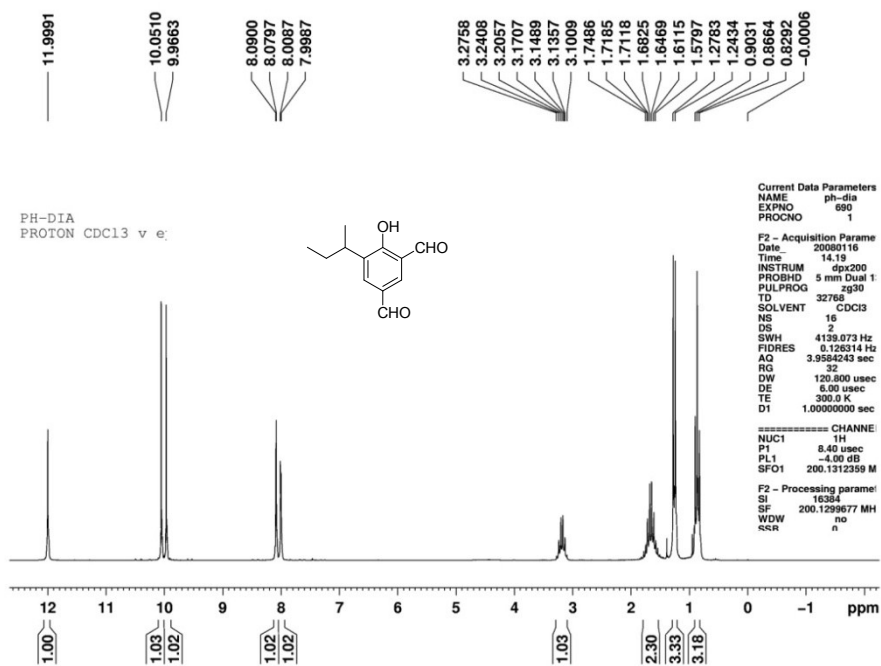
^1H NMR of compound **7** at 300 MHz (CDCl_3)



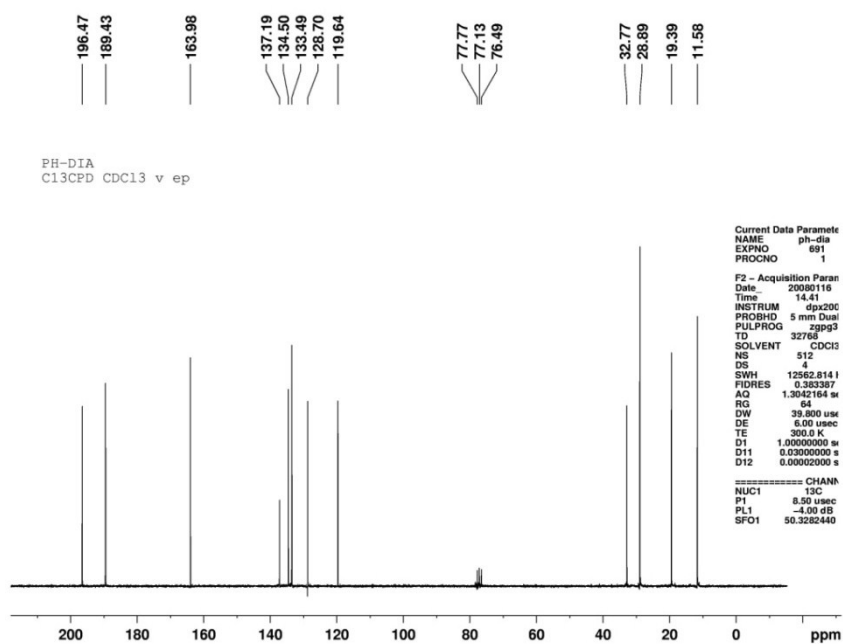
^{13}C NMR of compound **7** at 75 MHz (CDCl_3)



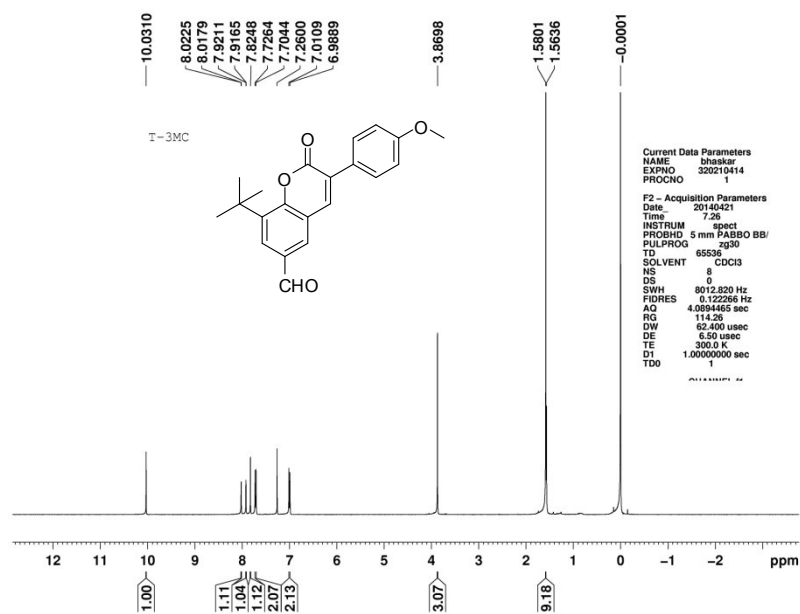
¹H NMR of compound **8** at 300 MHz (CDCl₃)



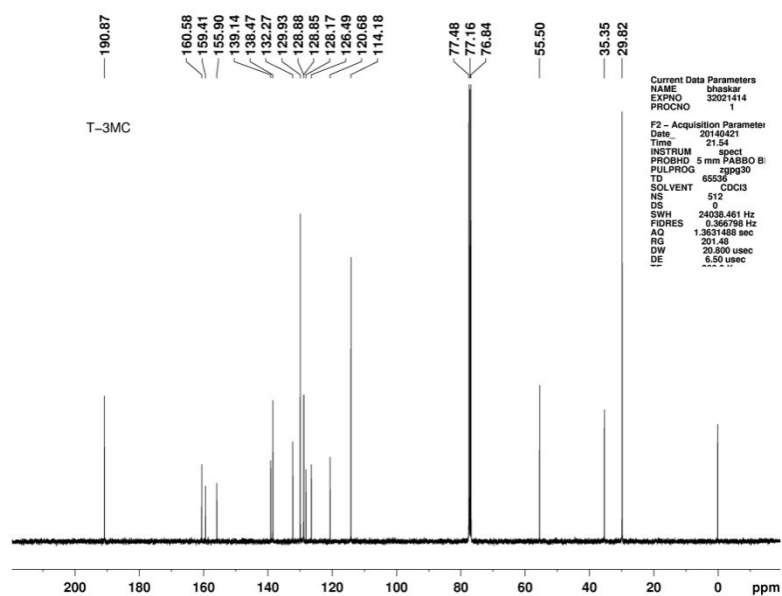
¹³C NMR of compound **8** at 50 MHz (CDCl₃)



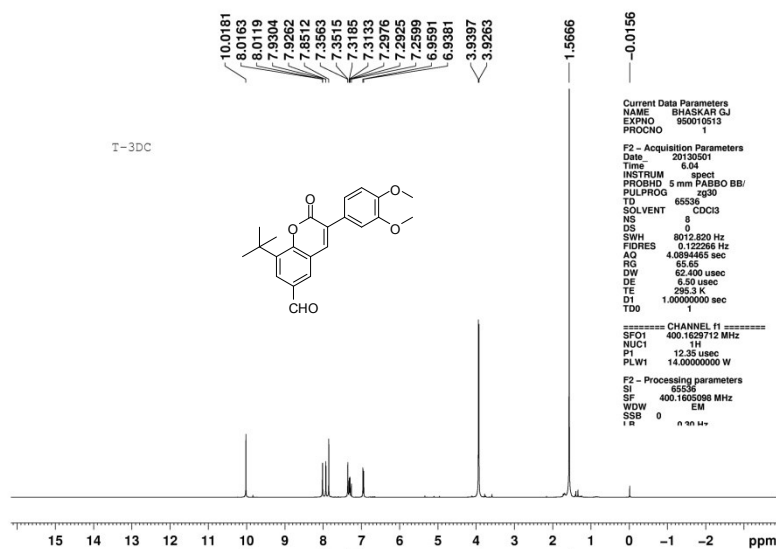
^1H NMR of compound **9** at 400 MHz (CDCl_3)



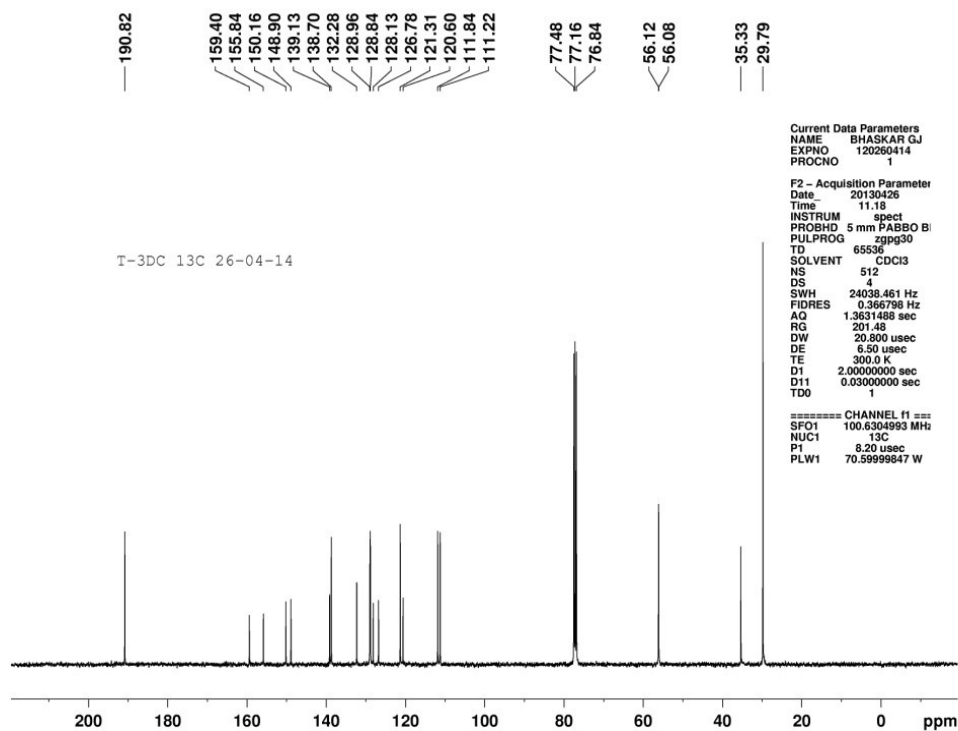
^{13}C NMR of compound **9** at 75 MHz (CDCl_3)



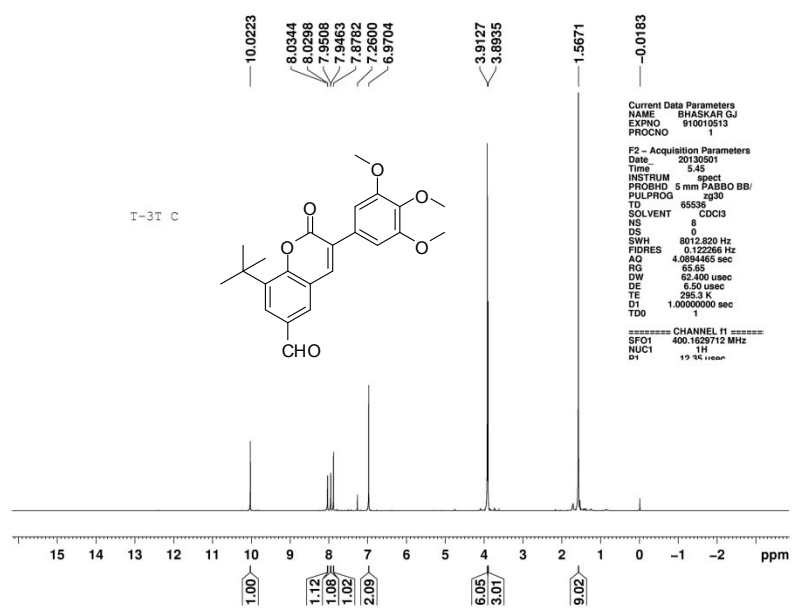
¹H NMR of compound **10** at 300 MHz (CDCl₃)



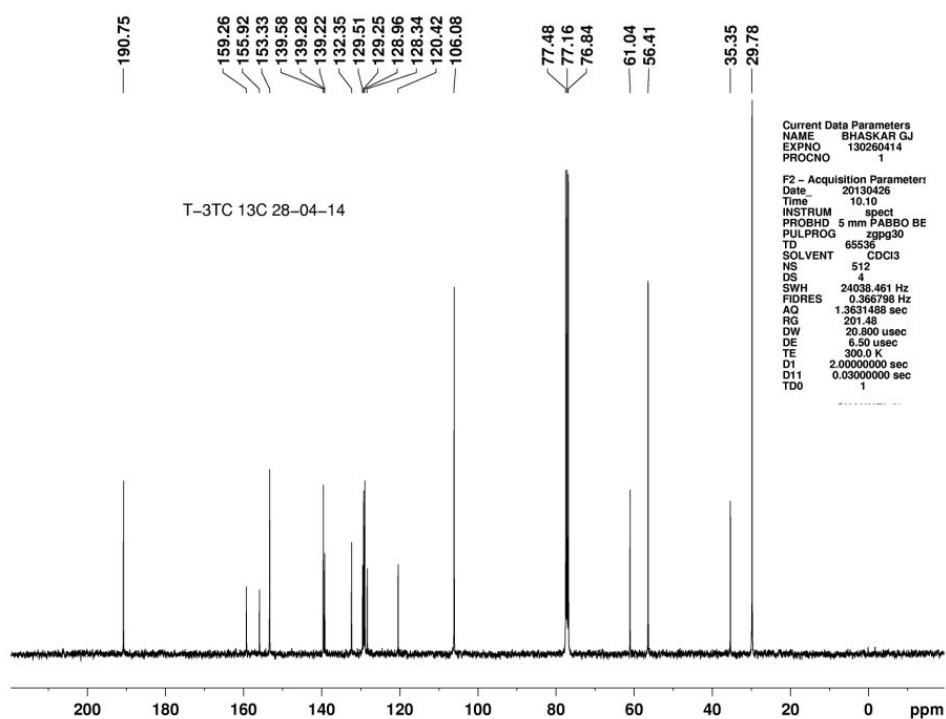
¹³C NMR of compound **10** at 100 MHz (CDCl₃)



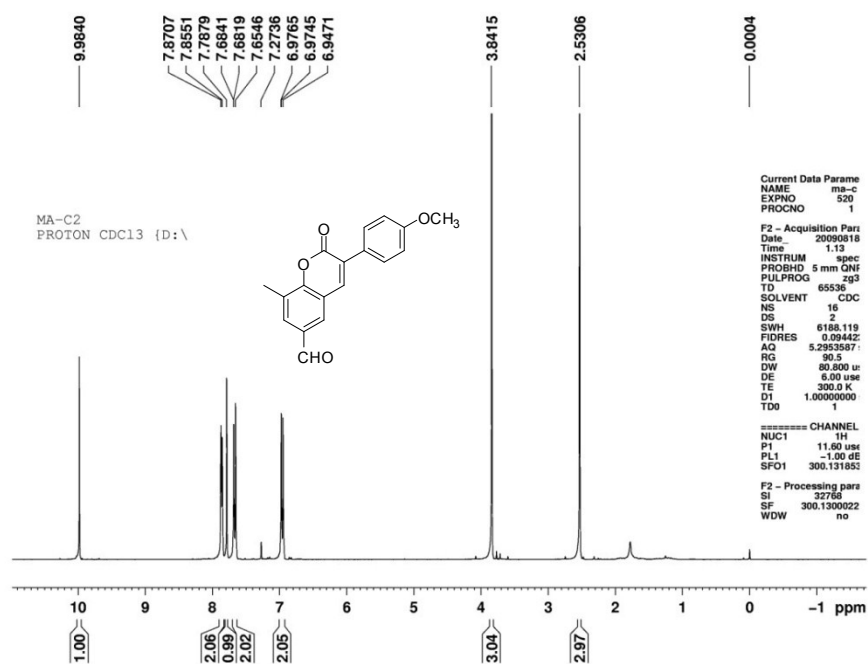
¹H NMR of compound **11** at 400 MHz (CDCl₃)



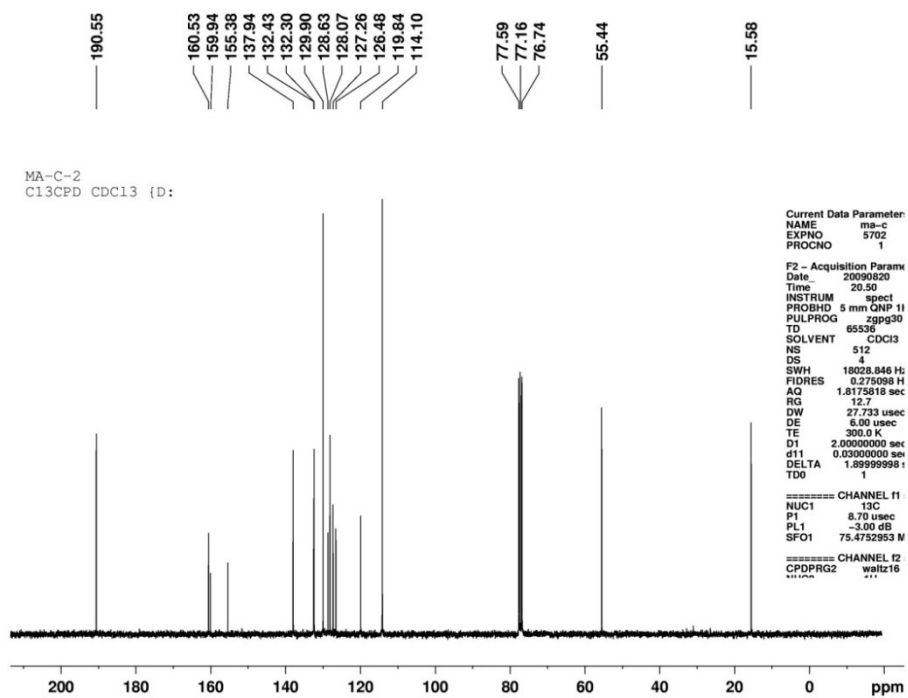
¹³C NMR of compound **11** at 100 MHz (CDCl₃)



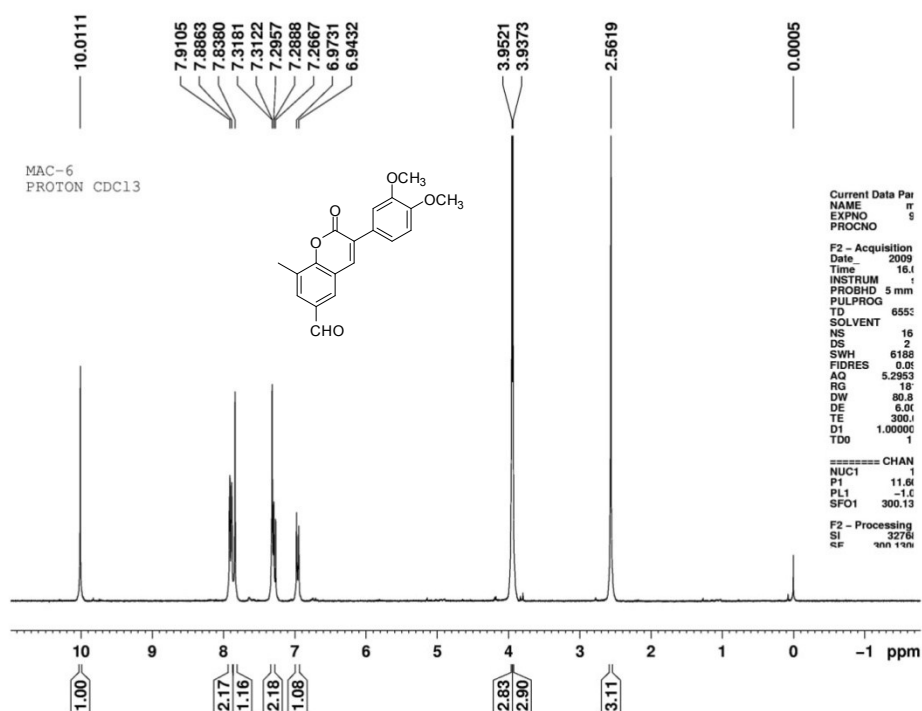
^1H NMR of compound **12** at 300 MHz (CDCl_3)



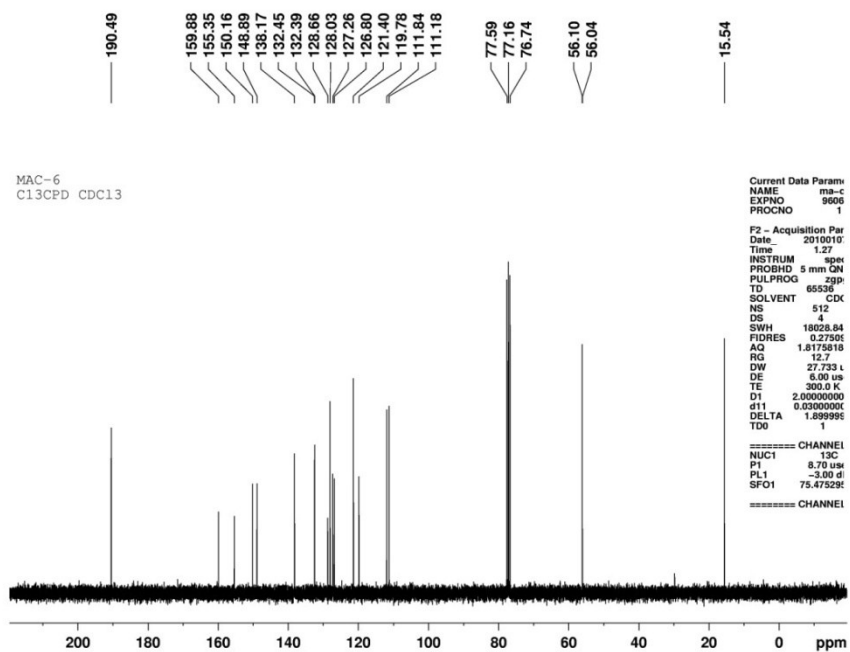
^{13}C NMR of compound **12** at 75 MHz (CDCl_3)



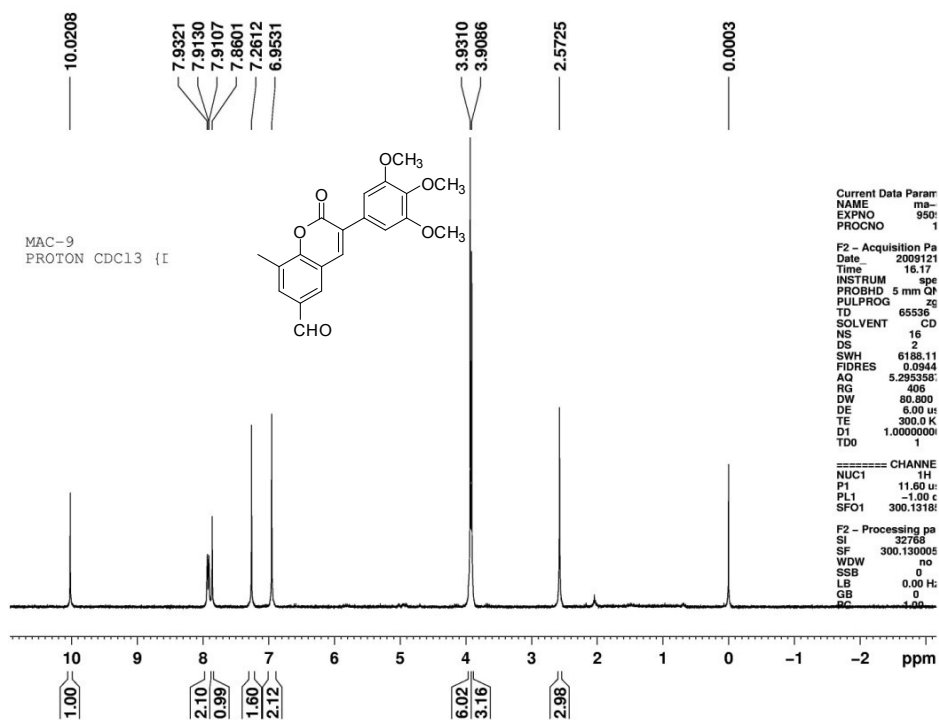
¹H NMR of compound **13** at 300 MHz (CDCl₃)



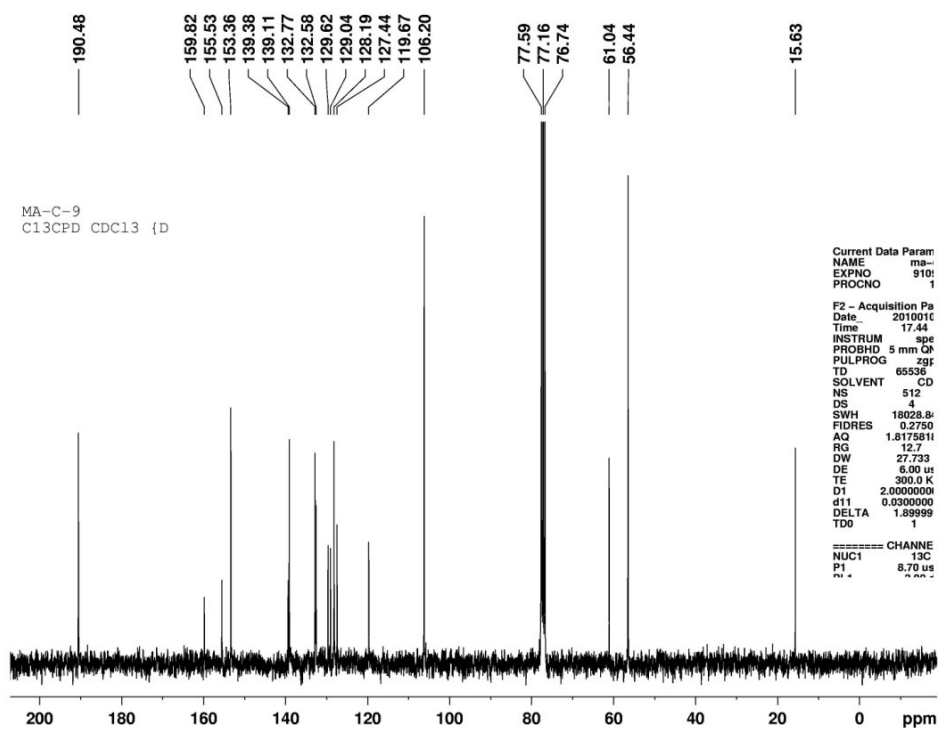
¹³C NMR of compound **13** at 75 MHz (CDCl₃)



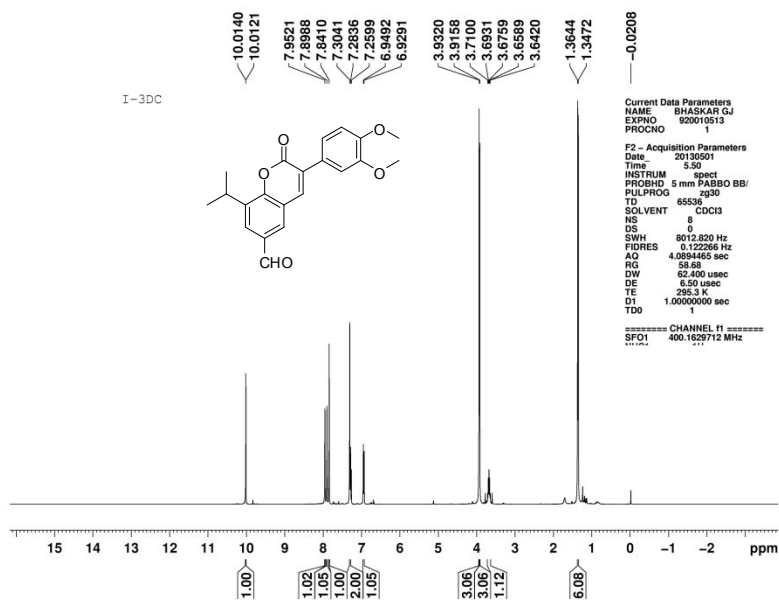
¹H NMR of compound **14** at 300 MHz (CDCl₃)



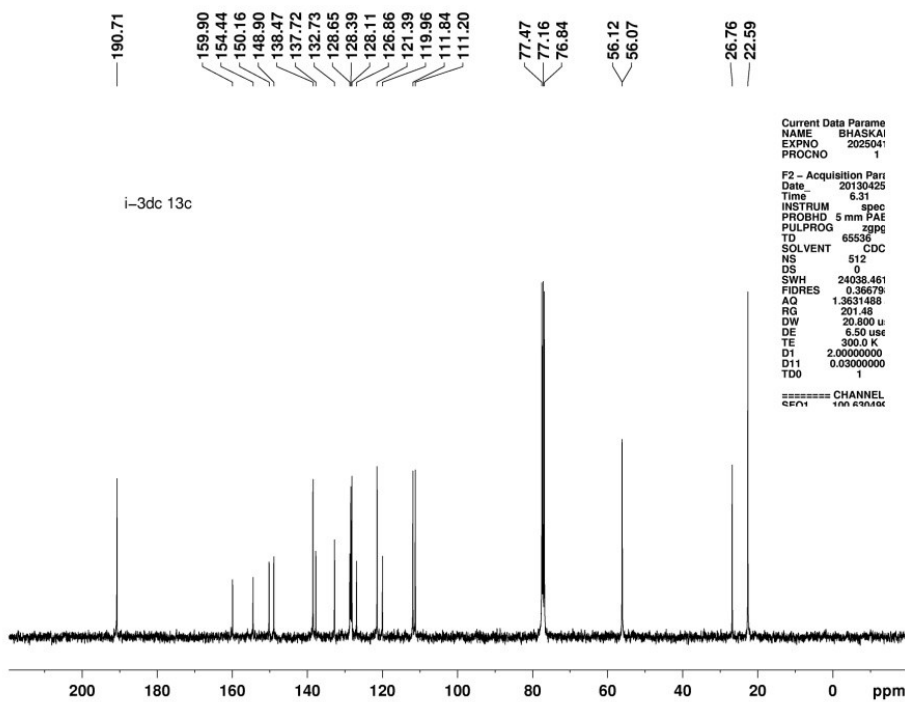
¹³C NMR of compound **14** at 75 MHz (CDCl₃)



^1H NMR of compound **15** at 400 MHz (CDCl_3)

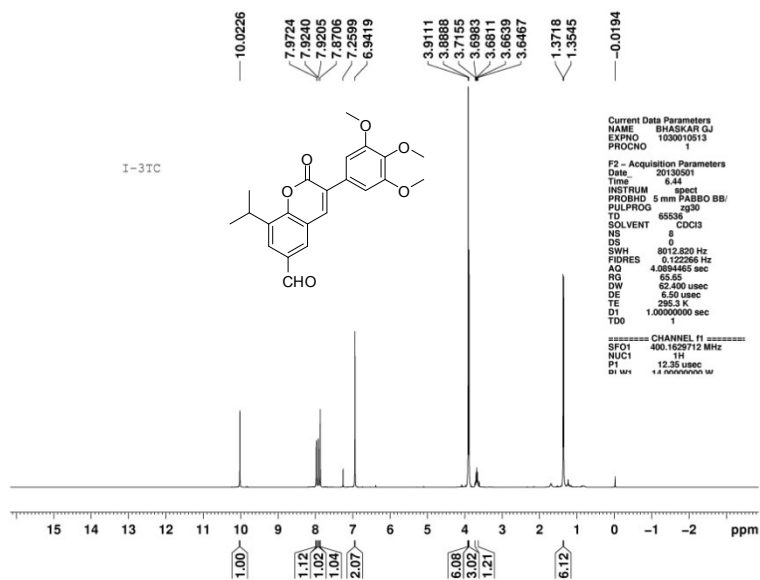


^{13}C NMR of compound **15** at 100 MHz (CDCl_3)

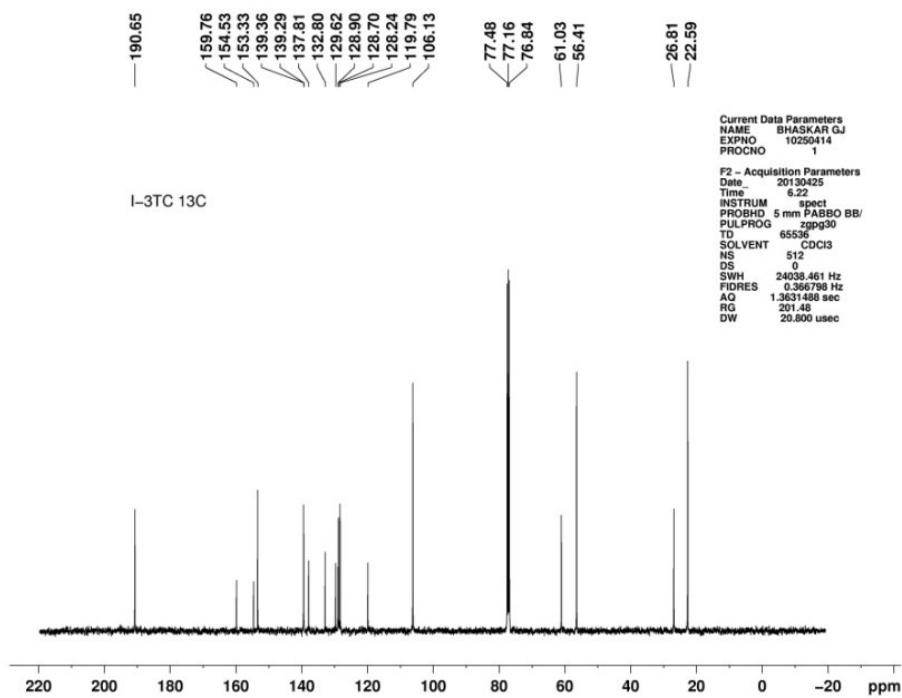


^1H
NMR

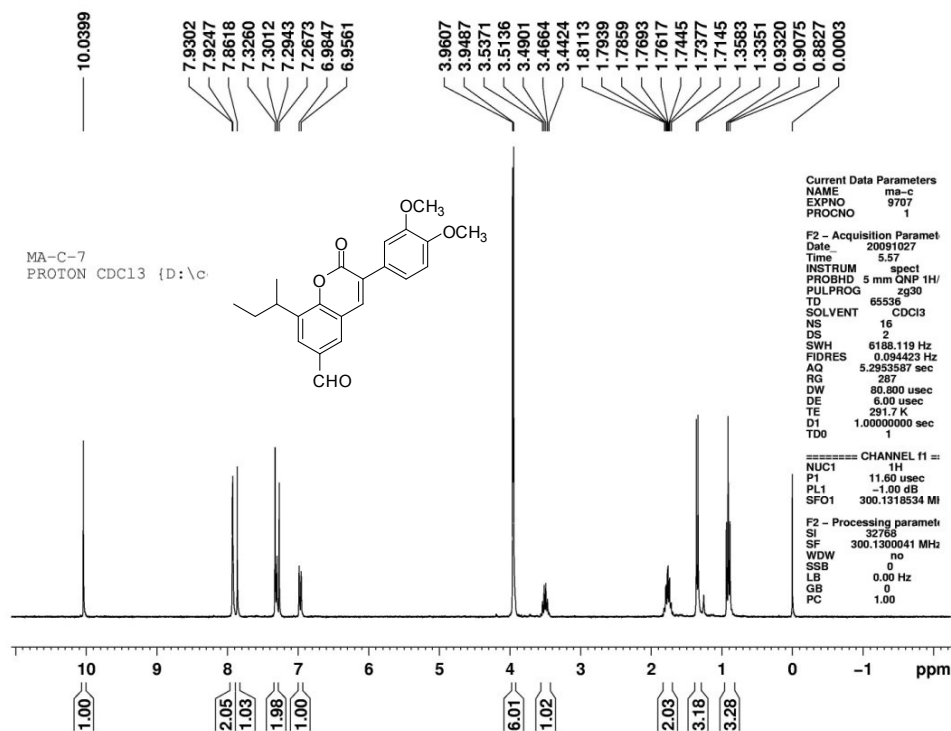
of compound **16** at 400 MHz (CDCl₃)



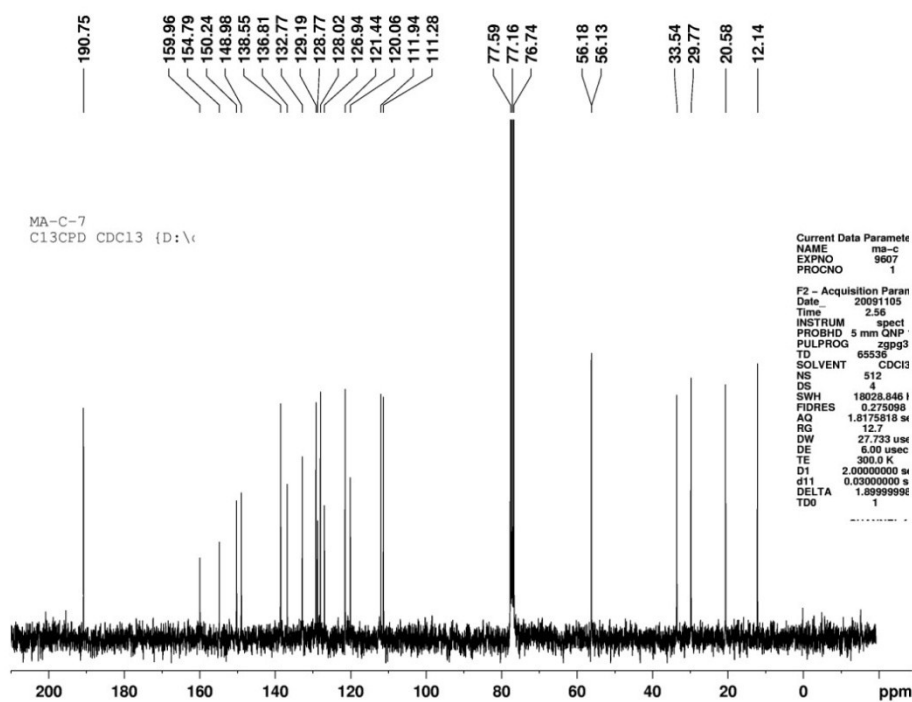
¹³C NMR of compound **16** at 100 MHz (CDCl₃)



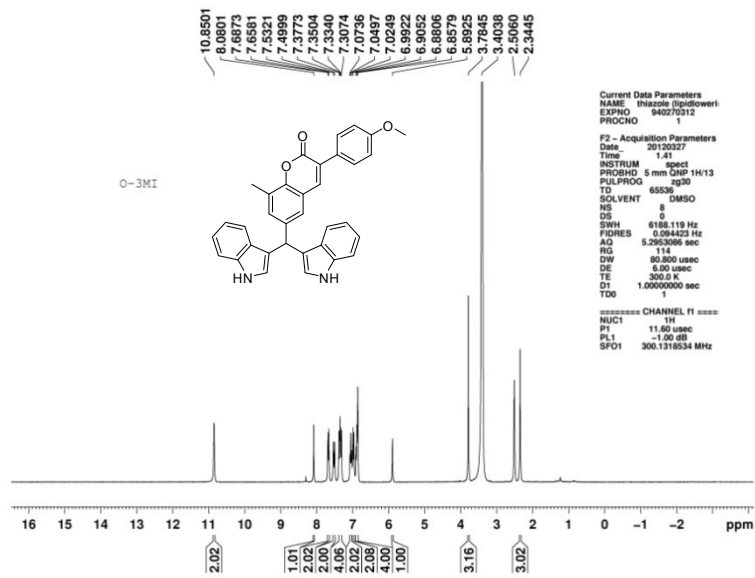
¹H NMR of compound **17** at 300 MHz (CDCl₃)



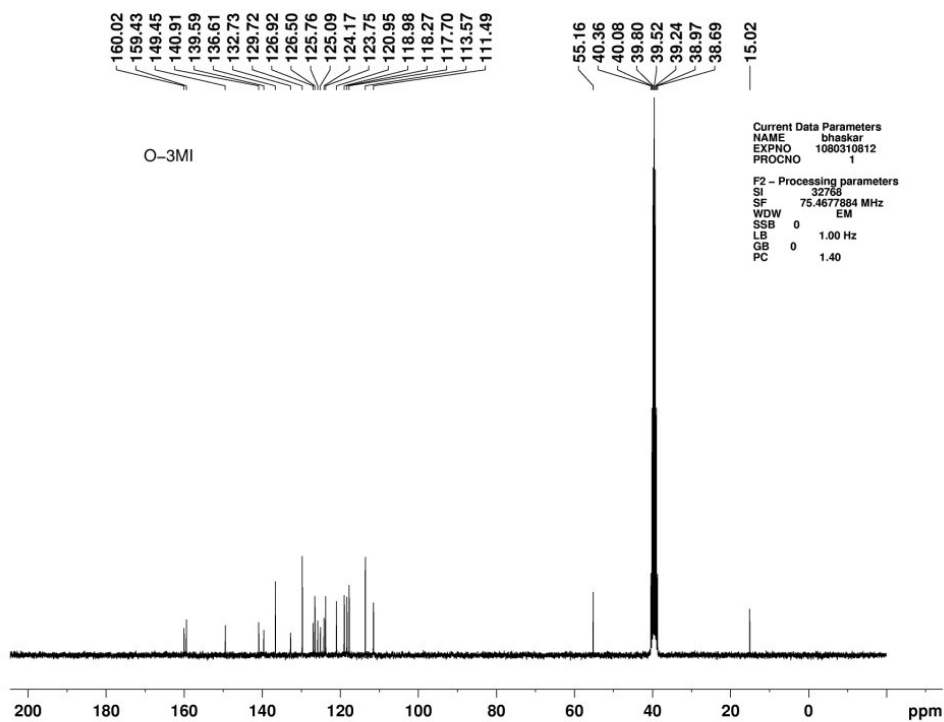
¹³C NMR of compound **17** at 75 MHz (CDCl₃)



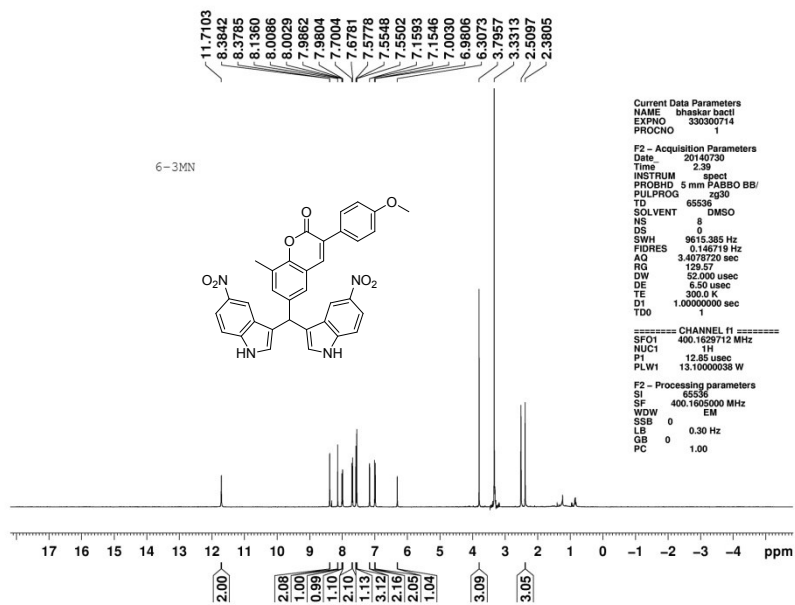
^1H NMR of compound **18** at 300 MHz (DMSO- d_6)



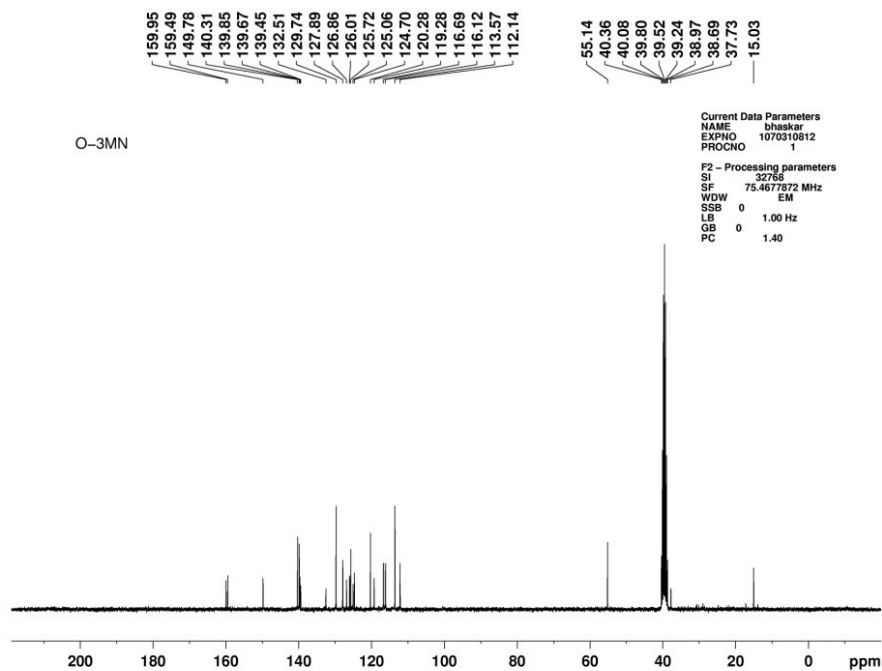
^{13}C NMR of compound **18** at 75 MHz (DMSO- d_6)



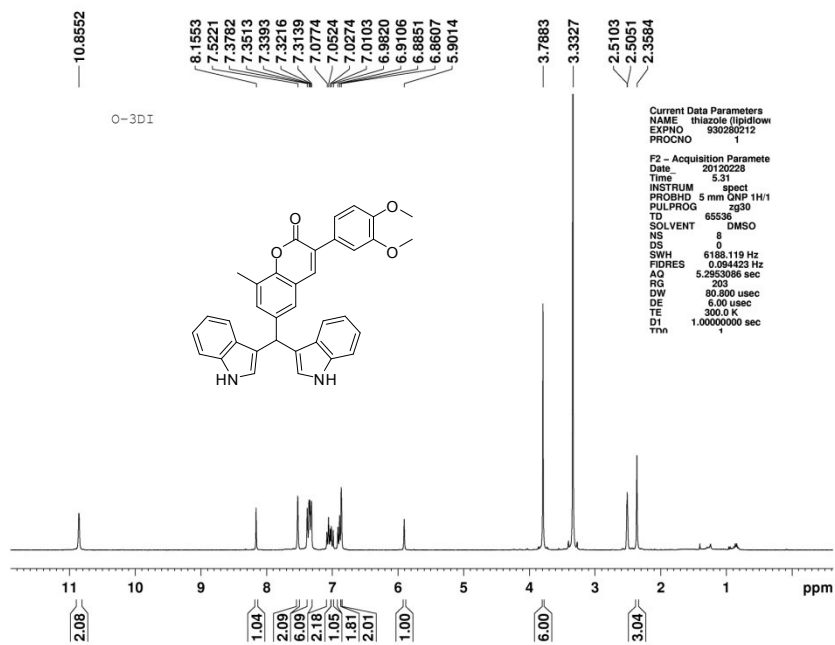
^1H NMR of compound **19** at 400 MHz (DMSO- d_6)



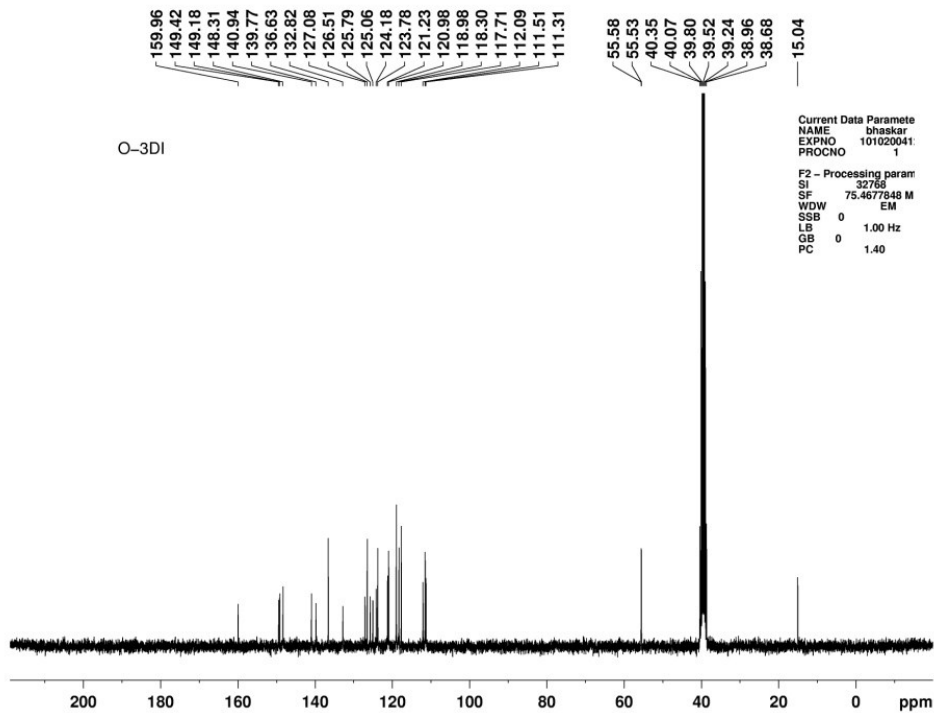
^{13}C NMR of compound **19** at 75 MHz (DMSO- d_6)



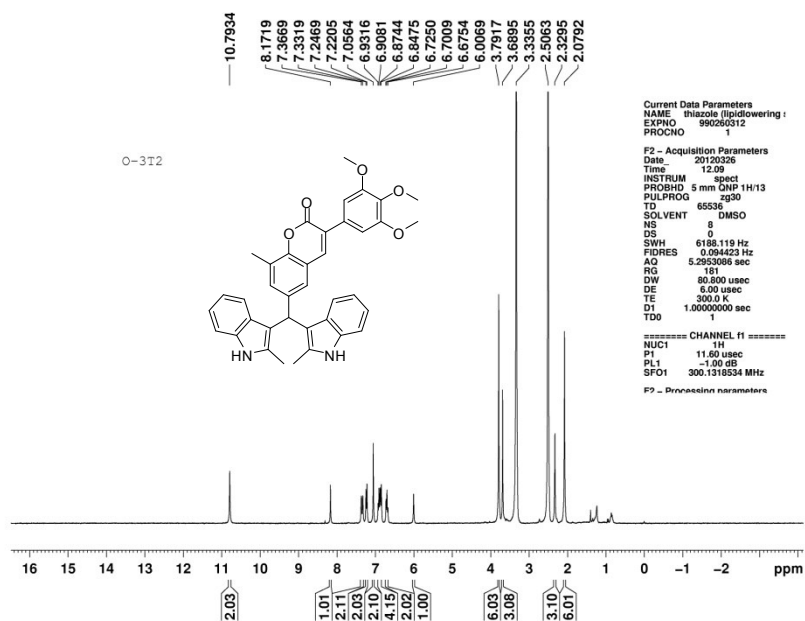
^1H NMR of compound **20** at 300 MHz (DMSO- d_6)



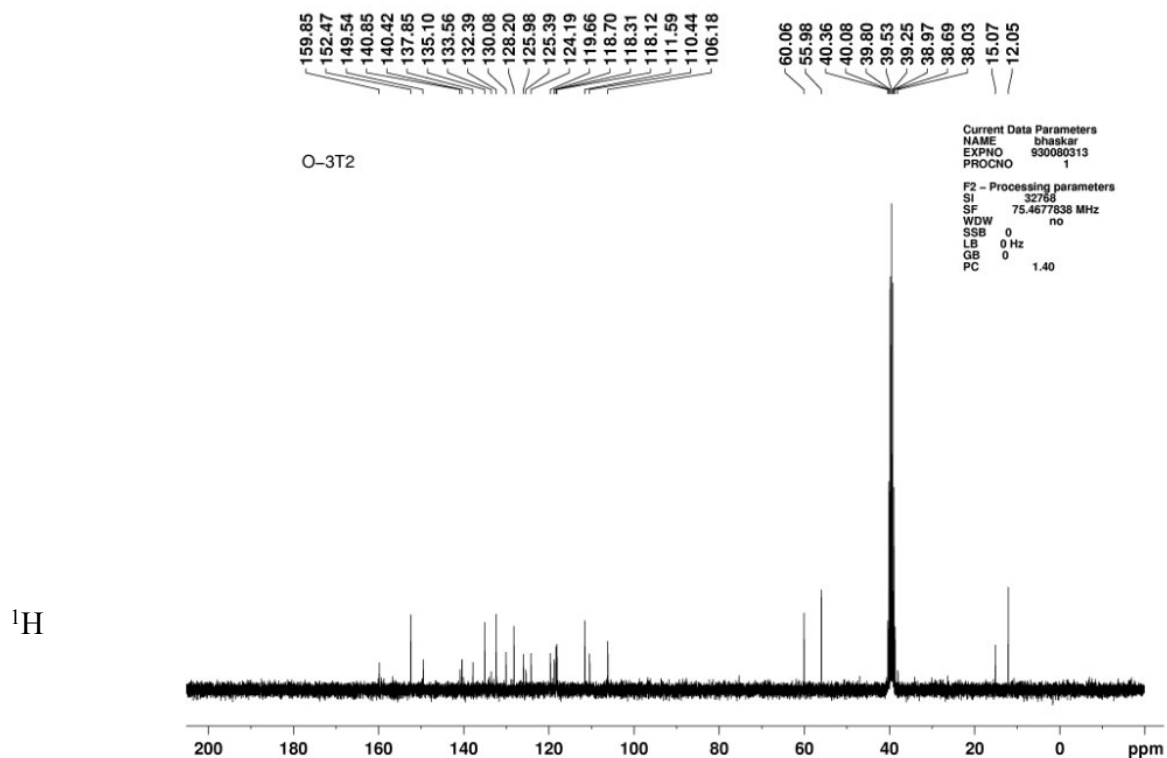
^{13}C NMR of compound **20** at 75 MHz (DMSO- d_6)



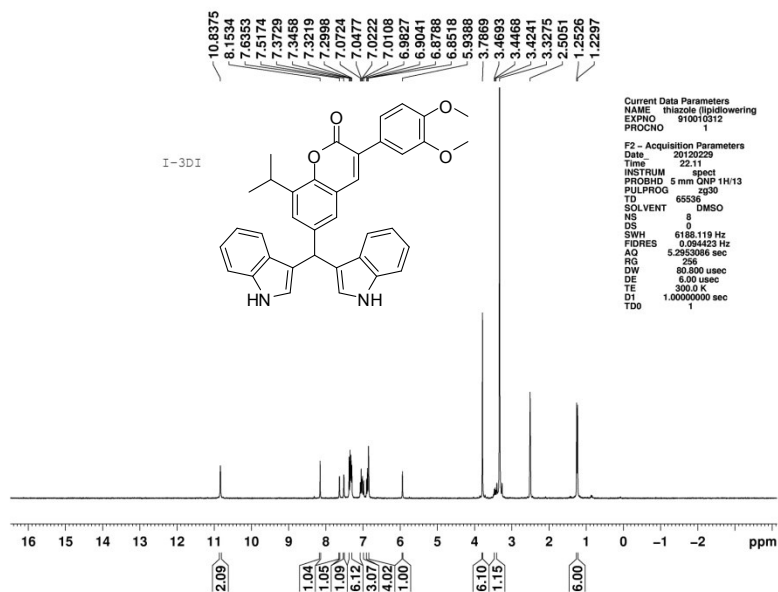
NMR of compound **21** at 300 MHz (DMSO- d_6)



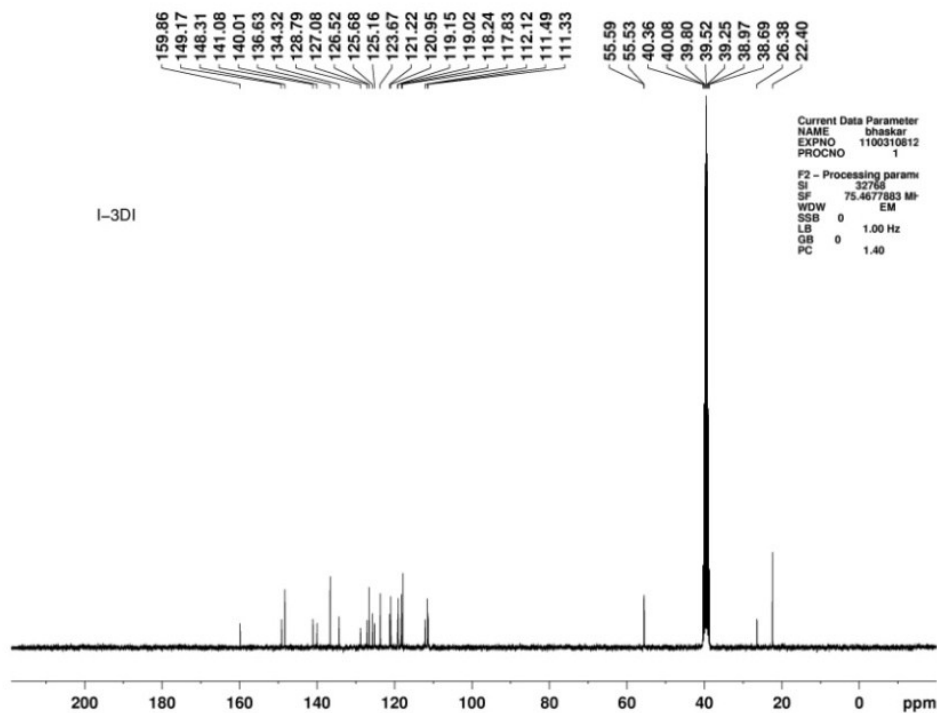
^{13}C NMR of compound **21** at 75 MHz (DMSO- d_6)



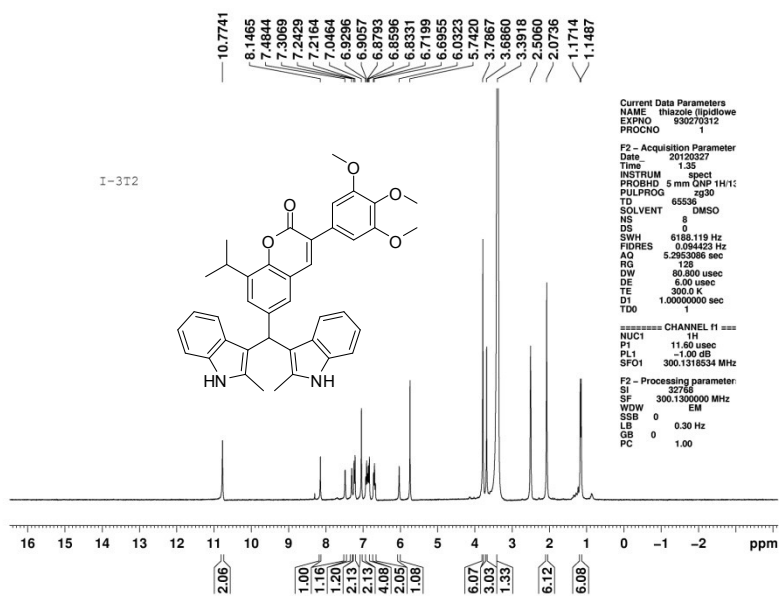
NMR of compound **22** at 300 MHz (DMSO- d_6)



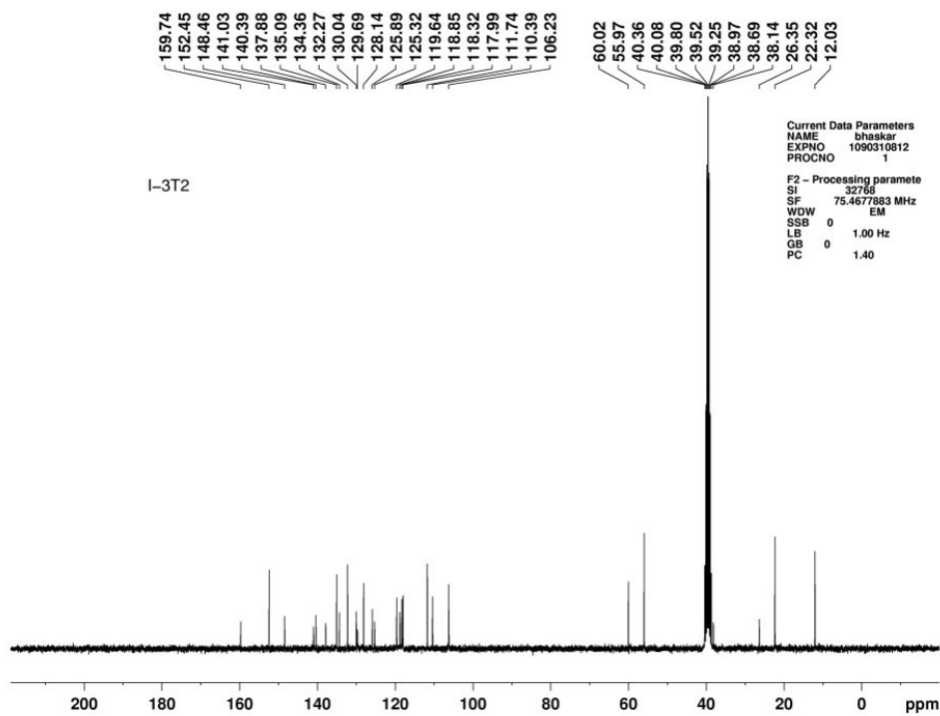
^{13}C NMR of compound **22** at 75 MHz (DMSO- d_6)



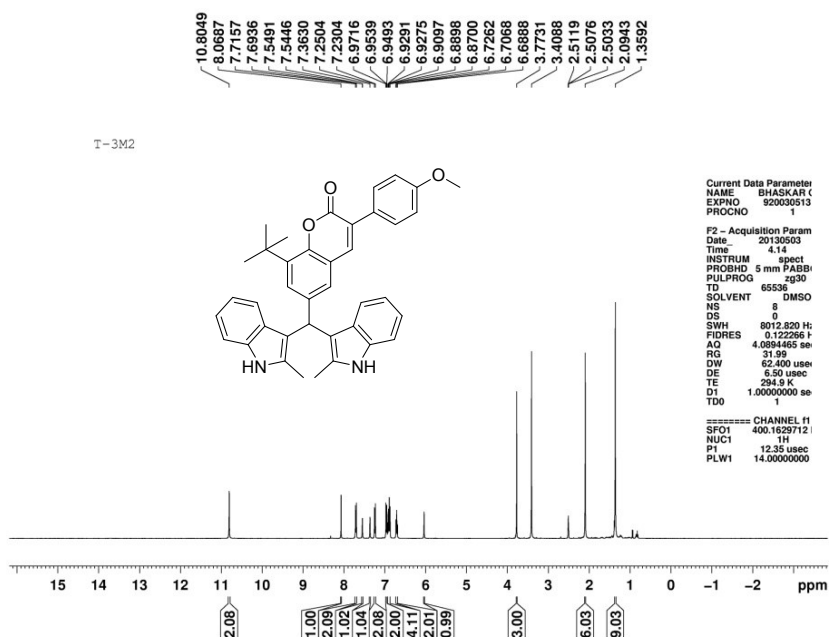
^1H NMR of compound **23** at 300 MHz (DMSO- d_6)



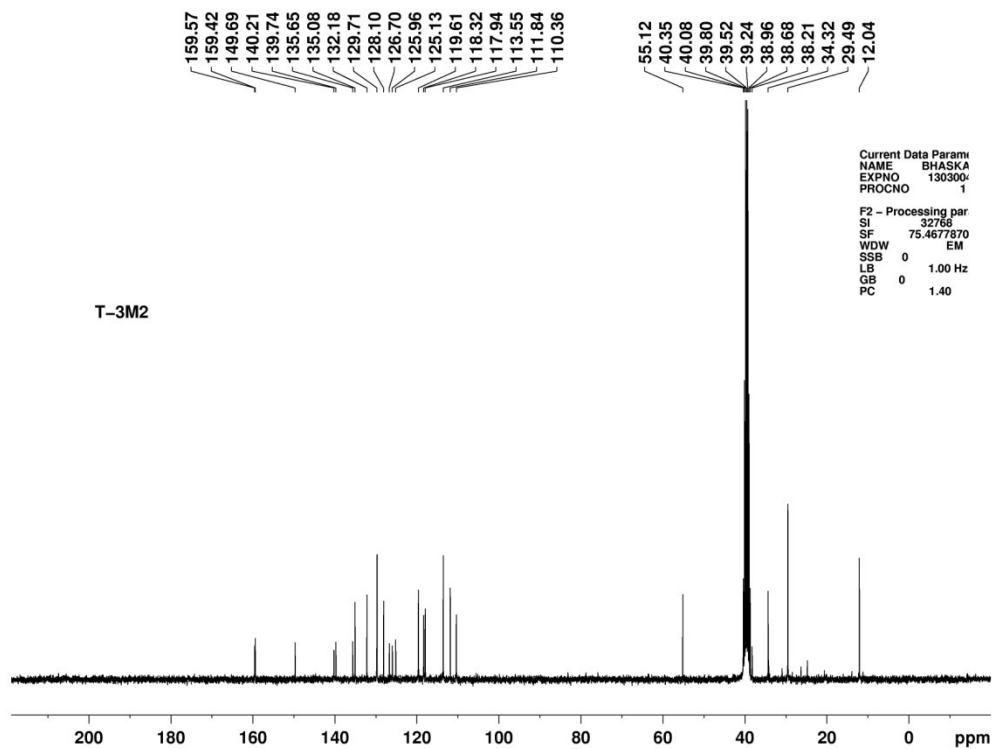
^{13}C NMR of compound **23** at 75 MHz (DMSO- d_6)



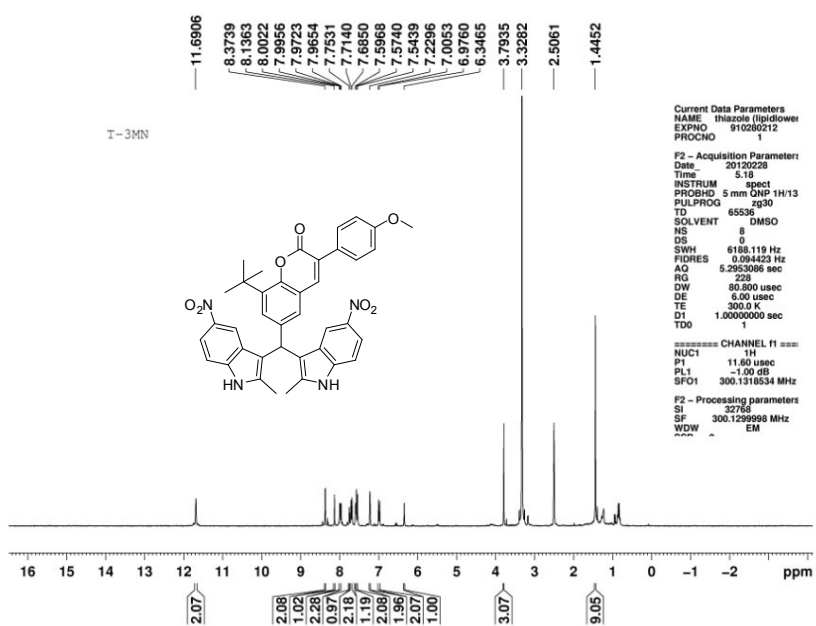
^1H NMR of compound **24** at 400 MHz (DMSO- d_6)



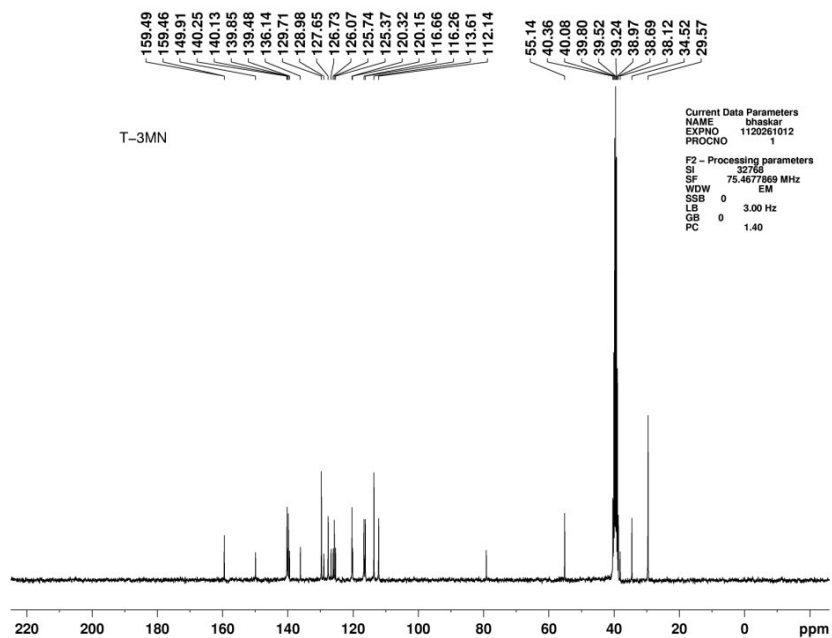
^{13}C NMR of compound **24** at 75 MHz (DMSO- d_6)



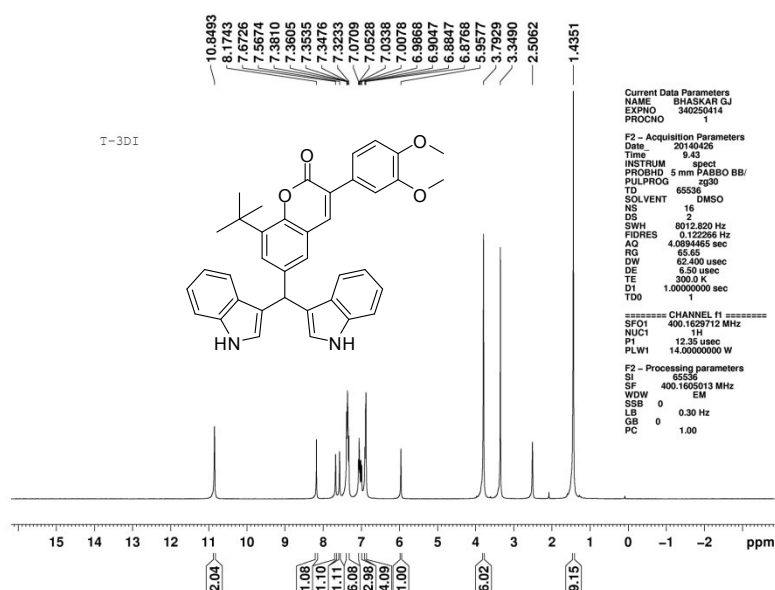
^1H NMR of compound **25** at 300 MHz (DMSO- d_6)



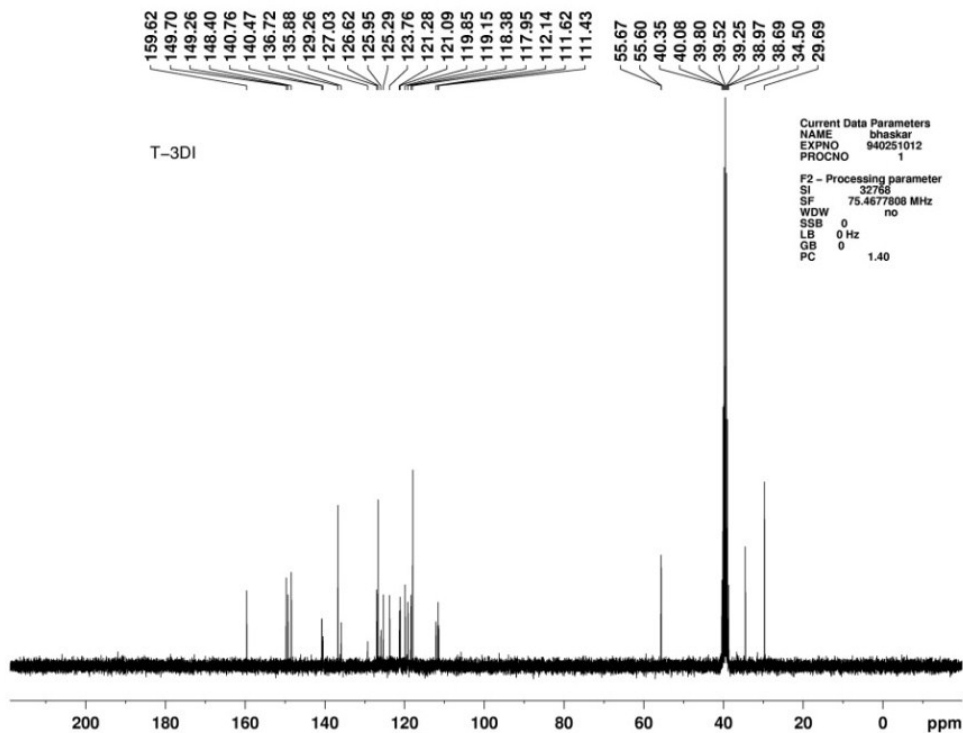
^{13}C NMR of compound **25** at 75 MHz ($\text{DMSO-}d_6$)



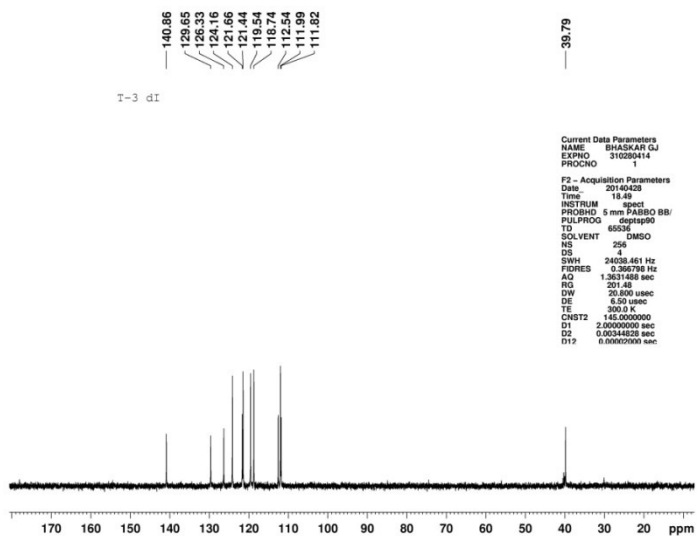
^1H NMR of compound **26** at 400 MHz ($\text{DMSO-}d_6$)



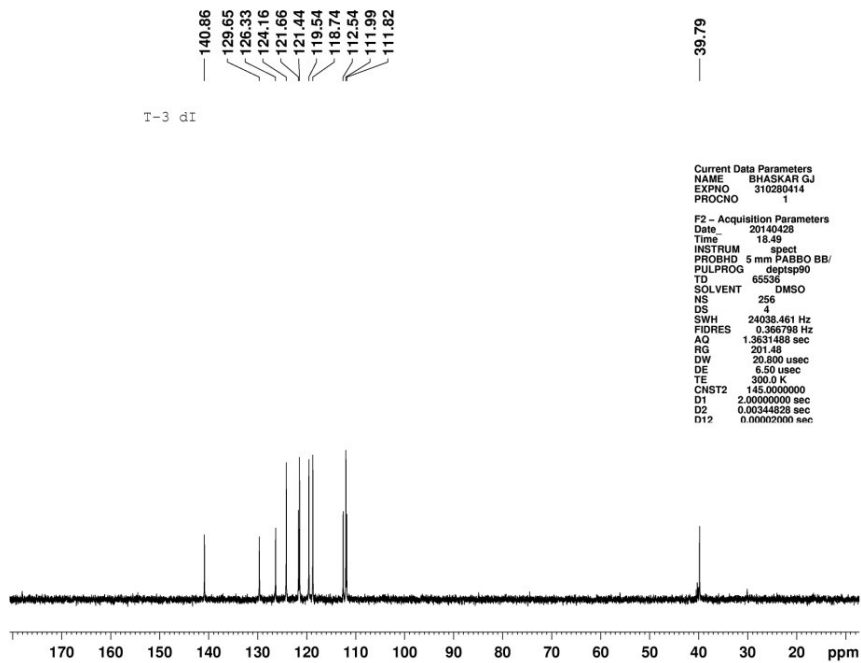
^{13}C NMR of compound **26** at 75 MHz (DMSO- d_6)



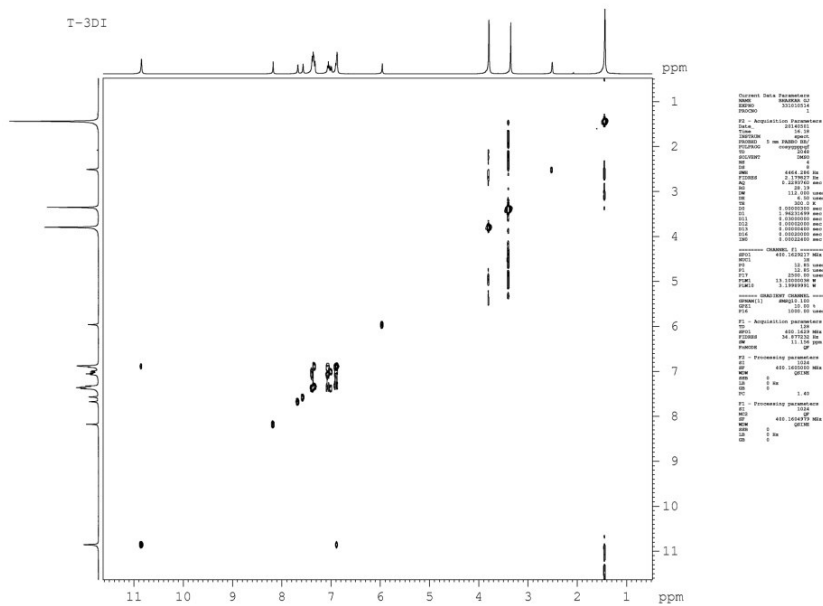
DEPT 90 of compound **26** at 100 MHz (DMSO- d_6)



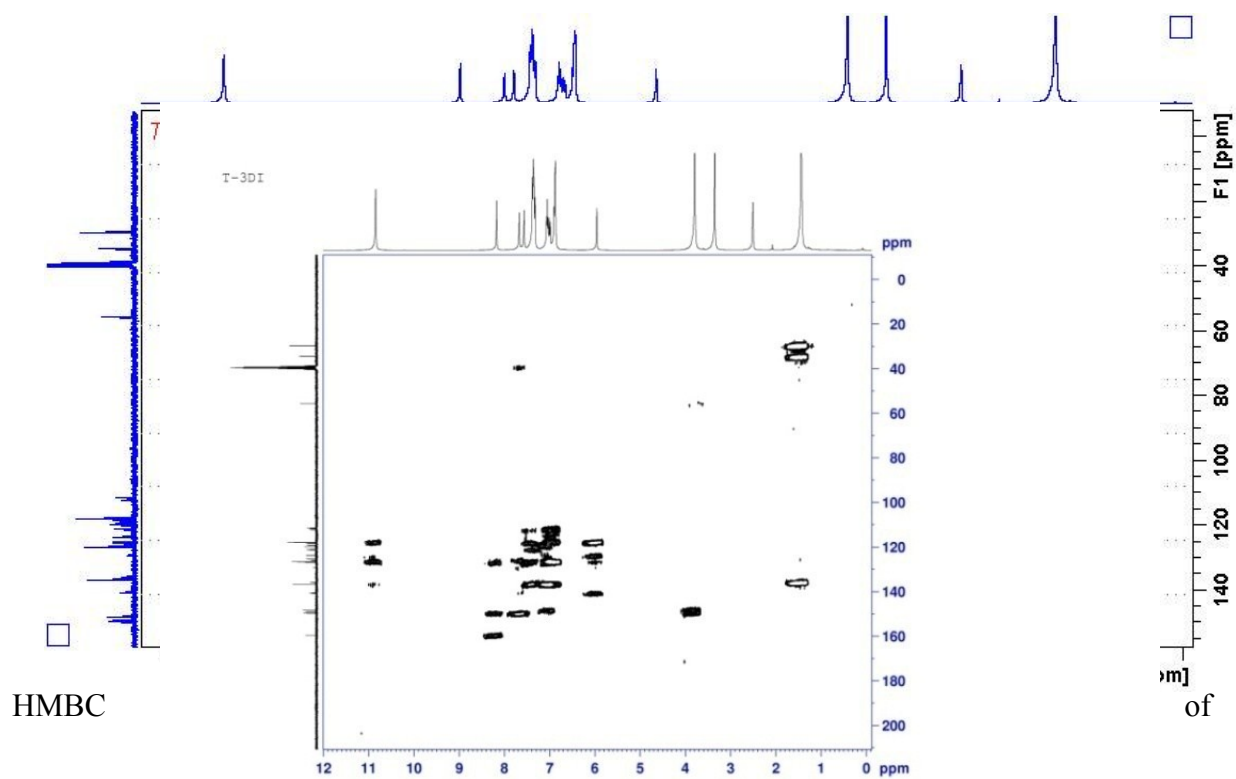
DEPT 135 of compound **26** at 100 MHz (DMSO-*d*₆)



COSY of compound **26** at 400 MHz (DMSO-*d*₆)

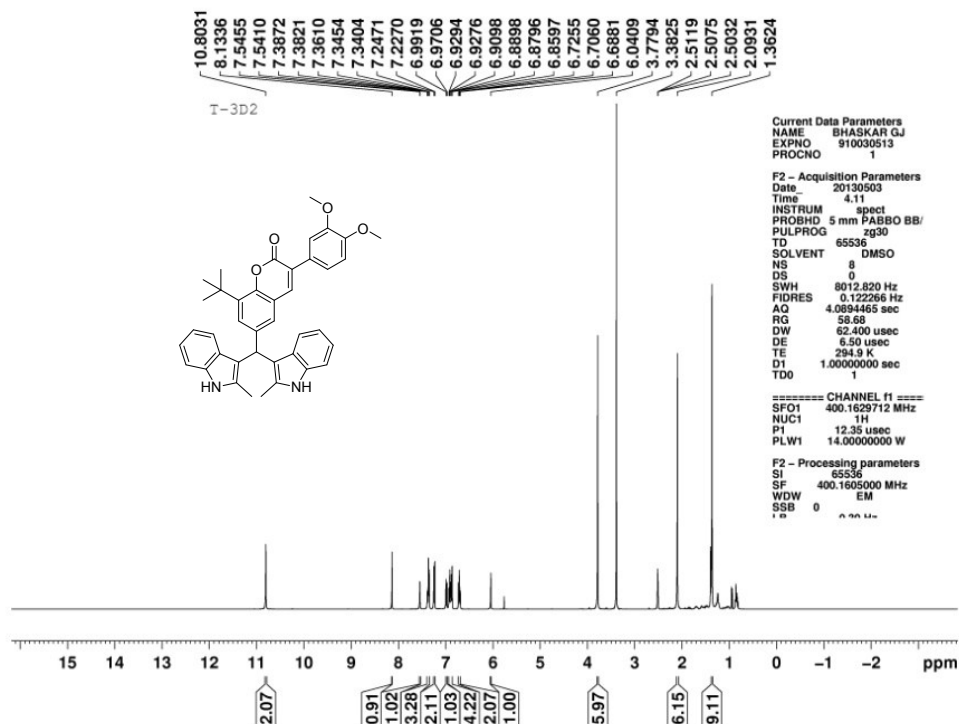


HSQC of compound **26** at 400 MHz (DMSO-*d*₆)

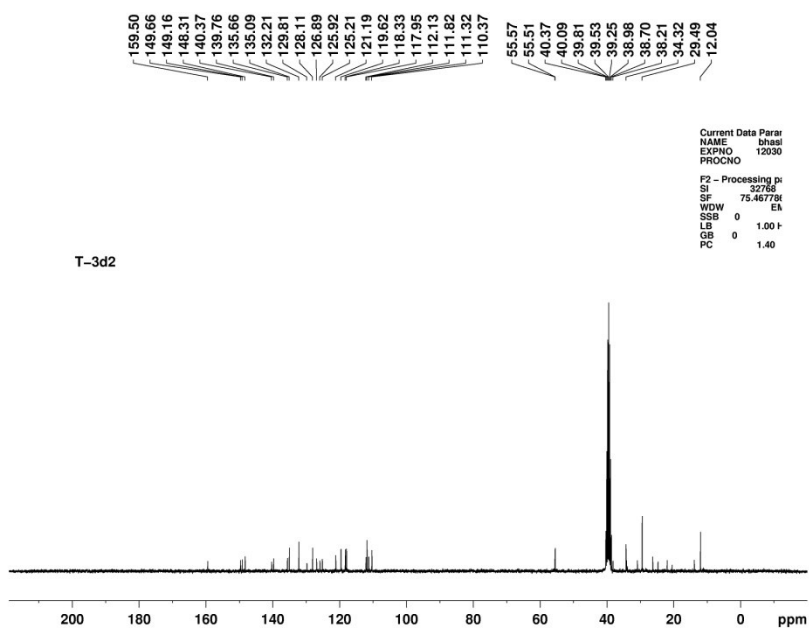


compound **26** at 400 MHz (DMSO-*d*₆)

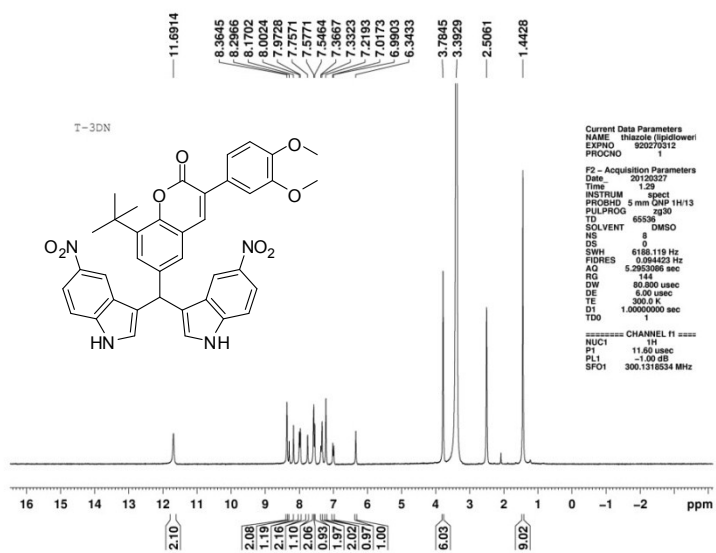
^1H NMR of compound **27** at 400 MHz (DMSO- d_6)



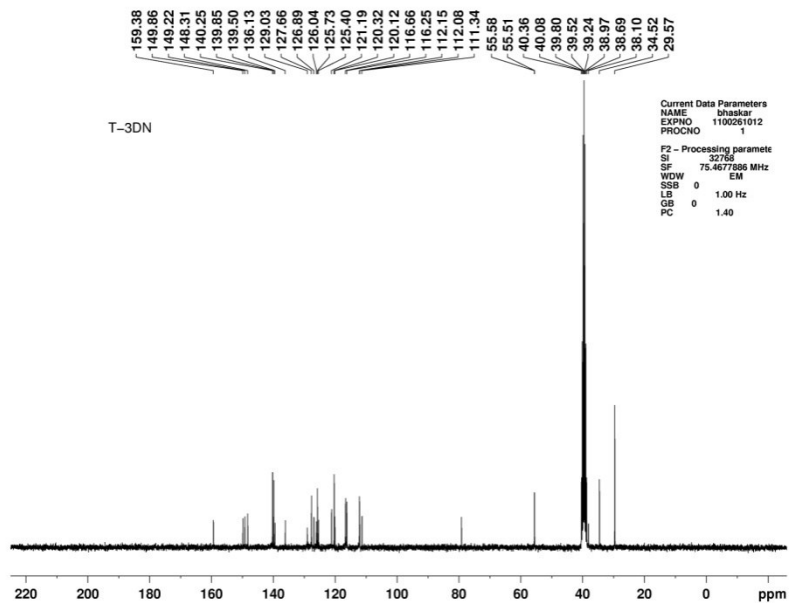
^{13}C NMR of compound **27** at 75 MHz (DMSO- d_6)



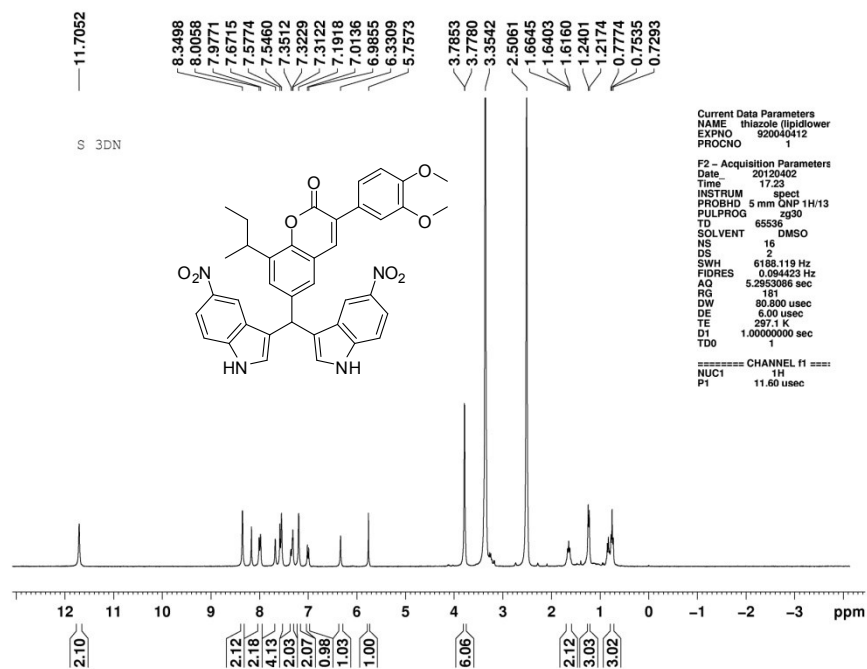
^1H NMR of compound **28** at 300 MHz (DMSO- d_6)



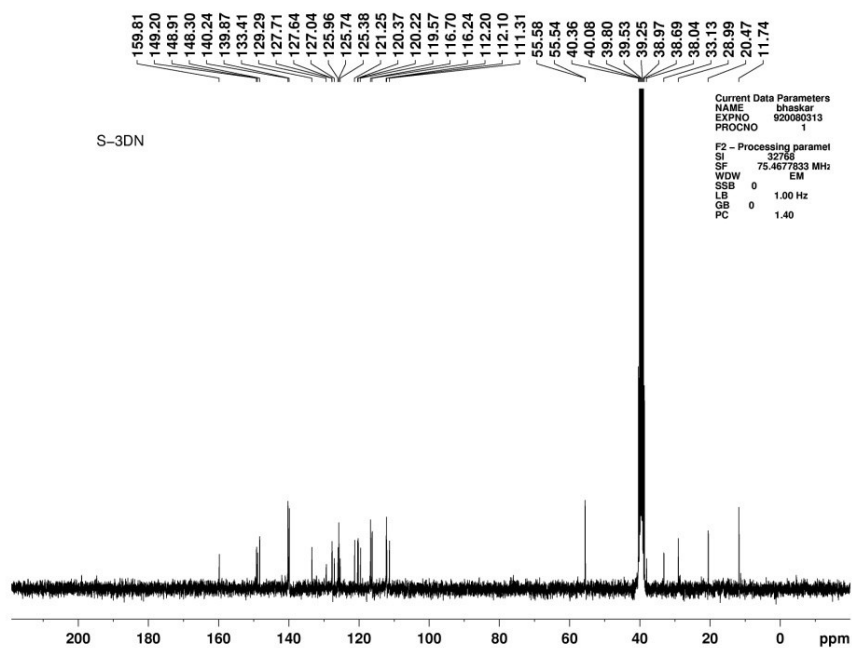
^{13}C NMR of compound **28** at 75 MHz (DMSO- d_6)



^1H NMR of compound **29** at 300 MHz (DMSO- d_6)



^{13}C NMR of compound **29** at 75 MHz (DMSO- d_6)



2. Bioanalytical LC-MS/MS method for compound 26

A Shimadzu (Shimadzu, Japan) SIL series LC system equipped with a degasser (DGU-20A3), isopump (LC-20 AD) and column oven (CTO-10AS) along with an auto-sampler (SIL-HTc) was used to inject 20 μ L aliquots of the processed samples, preceded with a guard column. A better chromatograph with a Thermo C18 (5 μ , 4.6 X 150 mm) column, was obtained using methanol: 0.1 % FA in triple distilled water (80:20, v/v) at a flow rate 0.75 mL/min. The column oven temperature was maintained at 30 °C and the total LC run time was 5.0 min.

Mass spectrometric detection was performed on an API 4000 Q trap mass spectrometer (Applied Biosystems, Canada) equipped with an electro-spray ionization (ESI) source in positive mode. The MS/MS system was operated at unit resolution in the multiple reaction monitoring (MRM) mode, using ion precursor \rightarrow product ion combinations of 583.3 \rightarrow 466.0 m/z for compound 451 and 180.1 \rightarrow 138.1 m/z for phenacetin (IS). Compound dependant parameters set for GS and IS, were declustering potential (DP), 150 and 71 V; entrance potential (EP), 10 V for both; collision energy (CE), 47 and 23 eV; and collision exit potential (CXP), 10 and 12 V, respectively. The method was validated to meet the acceptance criteria of FDA guidance for the bioanalytical method validation.¹

3. Binding Characteristics of Compound 26 with Proteins

3.1. Bovine serum albumin (BSA) interaction of compound 26.

Serum albumin forms major soluble fraction of blood and assists in blood pH stabilization and colloidal osmotic pressure. It reversibly interacts with diverse array of exogenous and endogenous compounds like various drugs / pharmaceuticals, proteins and fatty acids assisting their transportation and disposition to specific target site in body.^{2,4} Bovine serum

albumin (BSA) is a globular protein and monomeric BSA (66 kDa) comprising 583 amino acid residues. Various studies have been showed that domains and sub domains of BSA are established by 17 pairs of disulphide bridges. Family member proteins of serum albumin exhibit high degree of structural and functional homology. Beside similar chemical composition BSA shows around 80 % structural homology with human serum albumin.^{5,7} Thus, BSA was selected as a model blood protein in current study and interaction of bioactive compound **26** was studied by fluorescence quenching and absorption spectroscopy.

3.2. Intrinsic fluorescence quenching

The intrinsic fluorescence quenching has been exploited to elucidate mode of interaction between compounds and protein. BSA excited with 280 nm showed characteristic peak around 343 nm. Decrease in emission fluorescence intensities were observed with successive addition of compound **26** as shown in Figure 6a which was described by the Stern-Volmer equation:⁸

$$F_0 / F = 1 + K_{sv}[Q] = 1 + K_q \tau_0 [Q]$$

F_0 shows fluorescence intensity of BSA and F represents the fluorescence intensities and after the addition of the compound **26**, K_{sv} and K_q represent, the dynamic quenching constant and the quenching rate constant respectively; concentration of compound added is given by $[Q]$. τ_0 is the average lifetime of the molecule without quencher and its value is considered to be 10^{-8} s.⁹ Figure 6b shows Stern-Volmer plot indicating a linear relationship within the experimental concentrations.

In present study, a K_{sv} , $10.0 \times 10^4 \text{ L mol}^{-1}$ (R, 0.9989) and K_q , $10 \times 10^{12} \text{ L mol}^{-1} \text{ s}^{-1}$ were observed for the bioactive compound **26**. In current study we reported a higher K_q value

which exceeded the maximum value of the scattering collision quenching constant (2.0×10^{10} Lmol⁻¹s⁻¹) of biomolecules¹⁰ suggesting that BSA-compound **26** interaction were initiated by a complex formation. Beside complex formation dynamic collisions also contribute to the fluorescence quenching as shown by dynamic quenching constant.

We also analyzed the difference absorption spectroscopy to confirm the static complex formation by BSA and compound **26**. The difference absorption spectrum of BSA – compound **26** complex and compound **26** and BSA absorption spectrum (at the same concentration) was found to be non superposed (Figure 7). Our results indicated that compound **26** form a ground state complex with BSA. Two peaks were observed with BSA absorption spectra and the change around 210 nm peak is thought to be due to alteration in the BSA peptide backbone conformation (helix coil transformation) whereas the change around 280 nm is associated with altered microenvironment of Trp and Tyr residues¹¹ Our results indicated that compound **26** forms a ground state complex with BSA associated with alteration in the conformation of BSA.

3.3. Binding constant and site

Static quenching was studied by Modified Stern-Volmer¹² equation:

$$F_0/\Delta F = \{1/(faKa[Q])\} + 1/fa$$

ΔF is the change in fluorescence intensities in the BSA alone and with added compound **26** respectively, $[Q]$ is the concentrations of added compound **26**, fa represent fraction of accessible fluorophores, and Ka is the effective quenching constant, Figure 6c shows the Modified Stern-Volmer plots. The dependence of $F_0/\Delta F$ on the reciprocal value of concentration $[Q]^{-1}$ was linear and the value of $(faKa)^{-1}$ was determined from the slop of equation. Equation for the equilibrium in static quenching between free and bound molecules can be illustrated as:¹³

$$\text{Log } (F_0-F)/F = \log K_a + n \log [Q]$$

Where, n indicates the number of binding sites.

Binding constant (K_a) and the binding sites (n) were calculated through the plot of $\log (F_0-F)/F$ versus $\log [Q]$ as shown in Figure 6d. We reported calculated K_a , $14.11 \times 10^4 \text{ L mol}^{-1}$ (R, 0.9963) and n , 0.94 (R, 0.9976). The association constant (K_a) calculated for the compound (10^5 L mol^{-1}) indicates that the compound **26** has strong binding affinity for albumin protein and the number of binding sites ($n=1$) suggesting that the compound **26** binds with BSA at single high affinity binding site and ground state complex is formed.

4. Biological Materials and Methods

4.1. Animals

In vivo experiments were conducted as per the guidelines provided by the animal ethics committee (IAEC) of the Central Drug Research Institute, Lucknow, India. Rats (Charles Foster strain, male, adult, body weight 200-225 g) were kept in a room with controlled temperature at 25-26 °C, humidity 60- 80% and 12/12 hours light/dark cycle (light on from 8.00 AM to 8 PM) under hygienic conditions. Animals were acclimatized for one week before starting the experiment. The animals had free access to the normal diet and water.

4.2. Triton induced hyperlipidemic rat model

Rats were divided into different groups- control, triton treated and triton plus coumarin-indole hybrids of treated containing six animals in each group. In the acute experiment of 18 hours, hyperlipidemia was developed by administration of triton WR-1339 (Sigma Chemical Company, St. Louis, MO, USA) at a dose of 400 mg/kg, b.w. intraperitoneally (i.p), to animals of all the treated groups with derivatives of coumarin-indole hybrids were macerated with gum acacia, suspended in water and fed simultaneously with triton at a dose of 100 mg/kg p.o. to the animals of treated groups, diet was withdrawn. Animals of control and triton group without treatment with derivatives of coumarin-indole hybrids were given same

amount of gum acacia suspension (vehicle). After 18 hours of treatment the animals were anaesthetized with thiopentone solution (50 mg/kg b.w.) prepared in normal saline and 1ml blood was withdrawn from retro-orbital sinus using glass capillary in EDTA coated tubes (3.0 mg/ml blood). The blood was centrifuged at 2500 x g for 10 minutes at 4°C and plasma was separated. Plasma was diluted with normal saline (ratio of 1:3) and used for analysis of TC, PL and TG by standard enzymatic methods.²⁴ After the confirmation of most active compounds in primary screening we further evaluate the activity of compound **19** and compound **26** in same model at different doses (50, 100 & 150 mg/kg b.w).

4.3. HFD and induced hyperlipidemic rat model

HFD was purchased from Research Diet Inc, New Brunswick USA, containing fructose (9% w/w), deoxycholic acid (0.45% w/w), cholesterol (0.45% w/w), powdered chow diet (64% w/w) and coconut oil (26% w/w). Animals were divided into four weight matched groups given ND and HFD; hyperlipidemia was induced in three groups by feeding them HFD for 30 consecutive days. After induction of hyperlipidemia, Coumarin-indole derivatives and atorvastatin were given by oral gavage to one HFD-fed groups (HFD + Compound **26**, and HFD + Atorvastatin group), and the same volume of the vehicle (0.2% Gum acacia) was given in other HFD and ND groups. After 30 days of treatment, rats were fasted over night. Blood was withdrawn from the retro-orbital plexus using a glass capillary in an EDTA coated tube (3 mg/mL blood). Thereafter, animals were sacrificed, and the liver was excised gently, washed with cold 0.15 M KCl, and kept at 4 °C until analysis. Blood was centrifuged to collect serum.

4.4. Analysis of serum biochemical parameters: (Serum lecithin cholesterol acyltransferase (LCAT) activity)

Serum was fractionated into very low density lipoprotein (VLDL), low density lipoprotein (LDL) and high density lipoprotein (HDL) by polyanionic precipitation methods^{15, 16}. Serums

as well as lipoproteins were analyzed for their TC, PL, TG and protein by standard procedures reported earlier.^{17a} Aspartate transaminase (AST) and alanine transaminase (ALT) were determined by using commercially available kits from serum (Span Diagnostic *Limited*, *Surat, India*). Serum lecithin: cholesterolacetyltransferase (LCAT) activity was measured using method reported earlier.^{17b}

4.5. Analysis of hepatic biochemical parameters

The liver was homogenized (10%, w/v) in cold 100 mM phosphate buffer at pH 7.2 and used for the assay of total lipolytic activity of LPL.¹⁸ The lipid extract of each homogenate prepared in CHCl₃/CH₃OH (2:1 v/v) was used for the estimation of TC, PL and TG.¹⁹ Human serum LDL was prepared and radio-labeled with I¹²⁵, and the binding of this I¹²⁵LDL with liver plasma membrane preparation was assayed as described previously.^{20, 21}

4.6. HMG-CoA activity *in vitro* and *in vivo*

The *in vitro* HMG-CoA reductase assay was performed using the HMG-CoA reductase assay kit from Sigma Aldrich. HMG-CoA (substrate), NADPH, assay buffer and enzyme HMGR were supplied with the assay kit. HMG-CoA reductase activity in rat liver was measured from the HMG-CoA/mevalonate ratio. HMG-CoA was determined by its reaction with hydroxylamine hydrochloride at pH 5.5 and subsequent colorimetric measurement of the resulting hydroxamic acid by formation of complexes with ferric salts at 540 nm. Mevalonate was estimated by reaction with the same reagent but at pH 2.1. The ratio between HMG-CoA and mevalonate is inversely proportional to HMG-CoA reductase activity.²²

4.7. Faecal bile acids test

The rat feces were collected from all experimental groups from the day of dosing over 30 days and processed for the cholic and deoxycholic acid estimation test.²³

4.8. Statistical evaluation

Data are expressed as the means \pm SD. The statistical significance of all data was determined by using t-tests (two-sided) and one-way analysis of variance (ANOVA) followed by the Newman–Keuls test under post hoc analysis for multiple comparisons. Values of $P < 0.05$ were considered to denote statistical significance.

4.9. Docking of compound 26 to co-crystallized conformation of atorvastatin

MarvinSketch was used to draw and generate the 3D-conformation of compound **26**.^{24, 25} Further, compound **26** was subjected to 1000 steps of steepest descent minimization in UCSFChimera. Crystal structure of HMG-CoA reductase complexed with atorvastatin²⁶ was used as receptor to perform docking simulation of compound using SurflexX module available in SybylX.²⁷ Using co-crystallized conformation of atorvastatin, self docking was performed to validate the docking protocol. After validation, 30 docked conformations of compound **26** were generated using the same parameters.

4.10. Stability in simulated gastrointestinal fluids

Simulated gastric fluid (SGF) and simulated intestinal fluid (SIF) were prepared according to the formulation described in the 26th United States Pharmacopeia. Compound (10 μ M) was incubated in SGF and SIF. Sampling were done at 0, 15, 30 and 60 min time points for the gastric stability experiment and at 0, 30, 60, 90, 120 min for the intestinal stability experiment. Reaction mixture was kept at less than 1% organic content. At each time point, 200 μ L of sample was taken and quenched with 200 μ L of ice cold methanol. The concentration of compound **26** was determined by LC-MS/MS.

4.11. *In vitro* metabolism with rat liver microsomes

The *in vitro* metabolism studies were performed in SD rat liver microsomes (RLM). The incubation was performed as described and all analyses were performed in triplicate.²⁸ The metabolism of compound **26** in rat liver microsomes was performed in a microcentrifuge tube at concentrations of 10 μ M. The reaction media contained 2.0 mg/mL microsomal protein,

1.0 mM nicotinamide adenine dinucleotide phosphate (NADPH), and 40 mM MgCl₂ was added to Tris-HCl buffer (50 mM, pH 7.4). Reaction mixtures were incubated at 37 °C and total reaction volume was 2.0 mL. The incubation without addition of NADPH was used as negative control. Immediately after fortification of analyte into the microsomal suspension containing NADPH, the sampling point for t = 0 was taken, and further sampling points were taken at 5, 10, 20, 30, 45, 60 and 90 min. 100 µL of samples were taken and mixed with 500 µL of ice cold methanol containing IS (400 µg/mL) in a 1.5 mL centrifuge tube. Samples were centrifuged at approximately 12,000x g for 15 min and 100 µL of the supernatant was transferred into an injection vial for LC-MS/MS analysis. The *in vitro* half life (t_{1/2}, min) intrinsic Clearance (CL_i) and Hepatic clearance were calculated as described previously.²⁹

In-vitro half life and intrinsic clearance was calculated using following equation:

$$T_{1/2} = \frac{0.693}{K(\text{min}^{-1})}$$

$$\text{Intrinsic Clearance (CL}_{int}) = k(\text{min}^{-1}) \times \frac{[V]_{\text{incubation}}(\text{mL})}{[P]_{\text{incubation}}(\text{mg})}$$

$$\begin{aligned} \text{Hepatic clearance (CL}_{int}) \\ = K(\text{min}^{-1}) \times \frac{[V]_{\text{incubation}}(\text{mL})}{[P]_{\text{incubation}}(\text{mg})} \times 45 \left(\frac{\text{mg}}{\text{g}} \text{ liver} \right) \times \frac{\text{gm of liver}}{\text{Kg of body wt}} \dots \\ \text{. (3)} \end{aligned}$$

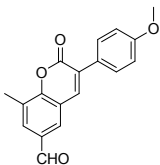
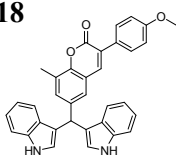
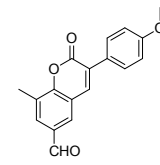
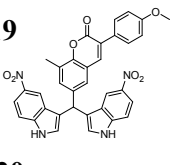
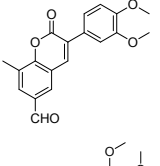
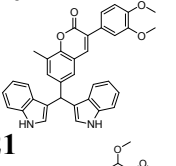
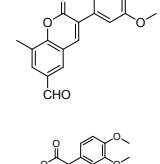
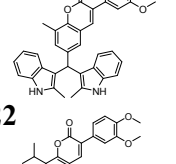
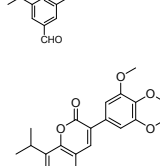
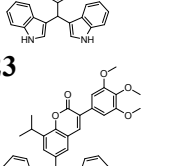
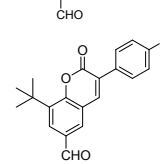
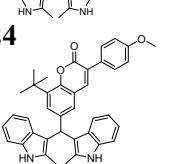
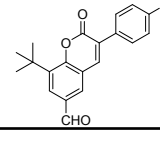
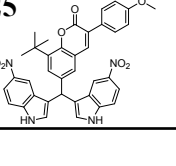


Where [V] is the incubation volume in mL and [P] is the amount of microsomal protein in the incubation mixture.

4.12. *In vivo* Pharmacokinetics studies in male Sprague–Dawley rats

In vivo pharmacokinetic study was performed in male Sprague–Dawley (SD) rats (n = 3, weight range 220–240 g) at a single oral dose of 100 mg/kg. Retro-orbital blood sampling was done from rats under mild ether anesthesia in microfuge tubes containing heparin as an anticoagulant at 0.25, 0.50, 1, 2, 4, 6, 8 and 12 h post dose administration. Plasma was

harvested by centrifuging the blood samples at 2000x g for 5 min and stored at -70 ± 10 °C until analysis. All experiments were carried out as per the guidelines of CPCSEA. Plasma sample (100 μ L) was processed using a protein precipitation technique employing 200 μ L of acetonitrile as a protein precipitant, and analysis was done using LC-MS/MS method to get the plasma concentration–time profile. Along with the plasma samples, quality control samples were distributed among calibrators and unknown samples.

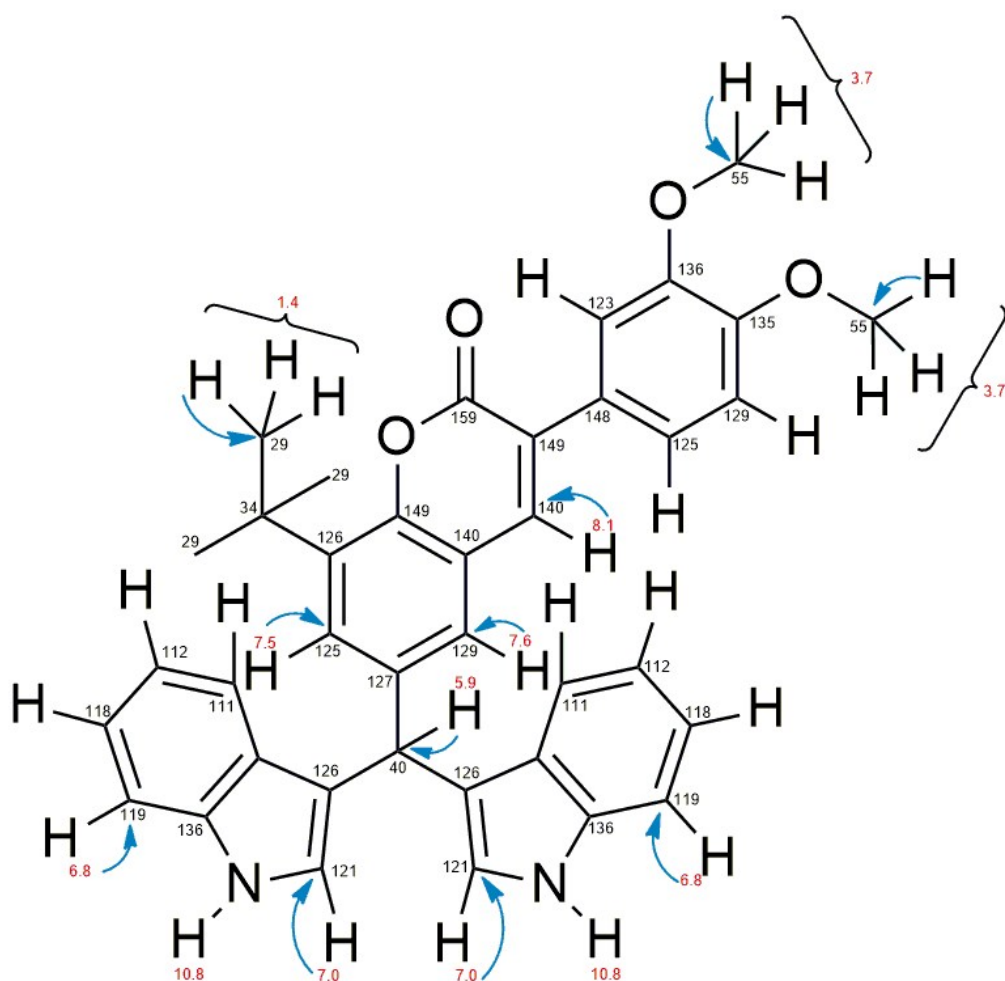
5. Yields of products 18-29

Entry	Reactant	Product	Time (min.)	Yield (%) ^a	mp (°C)
1		18 	30	68	168-169
2		19 	30	75	180-181
3		20 	30	73	155-156
4		21 	30	65	170-171
5		22 	30	75	180-181
6		23 	30	66	140-142
7		24 	30	69	253-254
8		25 	30	69	209-210

9		26		30	65	272-273
10		27		30	69	248-249
11		28		30	75	160-161
13		29		30	76	130-131

^aisolated yields.

6. HSQC correlations of compound 26



7. References

1. Human Services, Food and Drug Administration center for Drug Evaluation And Research Center(CDER) , Center for Veterinary Medicine (CVM) 2001.
2. M. Dockal, D.C. Carter, F. Ruker, *J. Biol. Chem.*, 2000, **275**, 3042-3050.
3. H.N. Tian, J.Q. Liu, J.Y. Zhang, Z.D. Hu, X.G. Chen, *Chem. Pharm. Bull.*, 2003, **51**, 579-582.
4. D.H. Ran, X. Wu, J.H. Zheng, J.H. Yang, H.P. Zhou, M.F. Zhang, Y.J. Tang, *J. Fluoresc.*, 2007, **17**, 721-726.
5. R. Kun, L. Kis, I. Dekany, *Colloids Surf. B Biointerfaces*, 2010, **79**, 61-68.
6. B. Liu, Y. Guo, J. Wang, R. Xu, X. Wang, D. Wang, L.Q. Zhang, Y.N. Xu, *J. Lumin.*, 2010, **130**, 1036-1043.
7. G.H. Xiang, C.L. Tong, H.Z. Lin, *J. Fluoresc.*, 2007, **17**, 512-521.
8. J. R. Lakowicz, 3rd edition. Springer, 2006, 11-12.
9. J.R. Lakowicz, G. Weber, *Biochemistry-U.S.*, 1973, **12**, 4161-4170.
10. M.R. Eftink, C.A. Ghiron, *Anal. Biochem.*, 1981, **114**, 199-227.
11. J. Jayabharathi, V. Thanikachalam, R. Sathishkumar, K. Jayamoorthy, *J.Photochem. Photobiol. B.*, 2012, **117**, 222-227.
12. S.S. Lehrer, *Biochemistry-U.S.*, 1971, **10**, 3254-3263.
13. A. Gong, X. Zhu, Y. Hu, S. Yu, *Talanta*, 2007, **73**, 668-673.
14. D.R. Wing, D.S. Robinson, *Biochem. J.*, 1968, **109**, 841-849.
15. T. Nagasaki, Y. Akanuma, *Clin. Chim. Acta.*, 1977, **75**, 371-375.
16. M. Burstein, P. Legmann, *Monogr. Atheroscler.*, 1982, **11**, 1-131.
17. (a) A.K. Khanna, R. Chander, C. Singh, A.K. Srivastava, N.K. Kapoor, *Indian J. Exp. Biol.*, 1992, **30**, 128-130. (b) T. Nagasaki, Y. Akanuma, *Clin. Chim. Acta.*, 1977, **75**, 371-375.
18. D.R. Wing, D.S. Robinson, *Biochem. J.*, 1968, **109**, 841-849.

19. R. Chander, A.K. Khanna, N.K. Kapoor, *Phytother. Res.*, 1996, **10**, 508-511.
20. P.T. Kovanen, M.S. Brown, J.L. Goldstein, *J. Biol. Chem.*, 1979, **254**, 11367-11373.
21. V. Singh, S. Kaul, R. Chander, N.K. Kapoor, *Pharmacol. Res.*, 1990, **22**, 37-44.
22. A.V. Rao, S. Ramakrishnan, *Clin. Chem.*, 1975, **21**, 1523-1525.
23. E.H. Mosbach, H.J. Kalinsky, E. Halpern, F.E. Kendall, *Arch. Biochem. Biophys.* 1954, **51**, 402-410.
24. <http://www.chemaxon.com/products/marvin/marvinsketch/>
25. E.F. Pettersen, T.D. Goddard, C.C. Huang, G.S. Couch, D.M. Greenblatt, E.C. Meng, T.E. Ferrin, *J. Comput. Chem.*, 2004, **25**, 1605-1612.
26. E.S. Istvan, J. Deisenhofer, *Science*, 2001, **292**, 1160-1164.
27. Tripos Associates Inc., St. Louis, Missouri, USA, 2013.
28. S. Chanda, M. Bashir, S. Babbar, A. Koganti, K. Bley, *Drug Metab. Dispos.*, 2008, **36**, 670-675.
29. P. Baranczewski, A. Stanczak, K. Sundberg, R. Svensson, A. Wallin, J. Jansson, P. Garberg, H. Postlind, *Pharmacol. Rep.*, 2006, **58**, 453-472.